Agricultural Water Management 292 (2024) 108675

Contents lists available at ScienceDirect

Agricultural Water Management

journal homepage: www.elsevier.com/locate/agwat

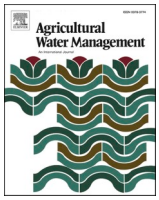

Advantageous spike-to-stem competition for assimilates contributes to the reduction in grain number loss in wheat spikes under water deficit stress

Juan Li [a], Zimeng Liang [a], Yakun Li [a], Kexin Wang [a], Vinay Nangia [b], Fei Mo [a], Yang Liu [a,1,*]

[a] College of Agronomy, Northwest A&F University, Taicheng Road 3, Yangling, Shaanxi 712100, PR China
[b] International Center for Agricultural Research in the Dry Areas (ICARDA), P.O. Box 6299–10112, Rabat, Morocco

ARTICLE INFO

Handling Editor - J.E. Fernández

Keywords:
Drought stress
Floret development
Source-to-sink relationship
^{13}C-photosynthate distribution
Sucrose utilization

ABSTRACT

This study was conducted to investigate the mechanisms of assimilate distribution and sugar metabolism in spike-stem that inhibit the formation of fertile florets and grains per spike in winter wheat under pre-reproductive drought stress. Two winter wheat cultivars, CH58 (relatively strongly drought tolerant) and LH6 (relatively weakly drought tolerant), were subjected to successive soil drought treatments from jointing to heading during the 2020–2022 growing seasons. The results showed that pre-reproductive drought stress intensified the degradation and abortion of wheat florets. Compared to CH58, the decrease in the number of fertile florets and grains per spike of LH6 under drought stress increased by an average of 5.3%−8.0% and 8.3%−9.0%, respectively. Drought significantly inhibited the distribution of ^{13}C-photosynthates in wheat spikes (15.7%−24.7%) and stems (8.5%−11.7%) during the booting stage. The number of differentially expressed genes enriched in starch and sucrose metabolic pathways was much higher in the spike and stem of LH6 than in those of CH58. Drought significantly reduced sucrose and hexose in young spikes but increased hexose and fructan concentrations in stems. Compared to LH6, the higher invertase activity and accompanying high expression of sugar transporter protein (*STP*) in CH58 spikes under drought stress contributed to the utilization of sucrose in young spikes. Additionally, under severe drought, the higher fructan concentration and expression of sugar transport proteins (*SWEET* and *SUT*) in the stem of CH58 improved the ability of the stem to transport assimilates to young spikes and thus alleviated the loss of grain number per spike. Exogenous spermidine optimized hexose and sucrose allocation in young wheat spikes and stems after drought stress, thereby increasing the number of fertile florets under drought stress. Overall, the ability of the dominant spike to utilize sugar and the ability to compete for assimilates between the spike and stem contribute to the resistance to drought stress-induced grain reduction in the spike. Exogenous chemicals can regulate the number of fertile florets through this pathway, thereby promoting the formation of wheat grain number.

1. Introduction

Drought events, which are worsened by climate change, pose a significant risk to food security both regionally and globally (Barnabas et al., 2008; Lobell et al., 2014; Gupta et al., 2020; Sheoran et al., 2022). Wheat, as one of the main food crops, mainly grows in arid and semi-arid regions of the world, and its production is significantly affected by the combined challenges of climate drought and water resource scarcity (Tian et al., 2023). Grains per spike is one of the key components of wheat yield, and it is the final manifestation of the development, degradation, and setting of wheat florets (Guo et al., 2016). There is a linear relationship between the number of fertile florets and grains per spike (Dreccer et al., 2014; Zhang et al., 2021). Therefore, it is essential to study the underlying mechanisms of the failure to form fertile florets and grain numbers per spike in wheat under sustained soil drought conditions, which will be crucial for future food security measures such as cultivation and/or molecular improvement under abnormal climate change conditions.

The period from jointing to booting is a crucial stage for wheat development and degradation. During this period, the meiotic and mitotic stages of floret development are highly susceptible to drought conditions (Yu et al., 2019). Although drought stress after floret

* Corresponding author.
E-mail address: liuyang0328@126.com (Y. Liu).
[1] ORCID: 0000-0003-1512-6362

https://doi.org/10.1016/j.agwat.2024.108675
Received 28 September 2023; Received in revised form 19 December 2023; Accepted 5 January 2024
Available online 13 January 2024

differentiation does not affect floret primordia, it significantly increases the rate of floret degradation and pollen sterility, thereby reducing the number of grains per spike (Dolferus et al., 2011; Dong et al., 2017; Danilevskaya et al., 2019). Among them, the process of floret development and degradation in relatively drought-sensitive varieties of wheat is significantly influenced by drought (Dong et al., 2017). However, its specific mechanism still needs further investigation.

The scarcity of available resources is a crucial factor that significantly impacts the developmental quality of florets. (Fischer, 2011; Zhang et al., 2020). The assimilates allocated to the young spike are primarily determined by the availability of carbohydrates provided by source organs and the competition between the young spike and stem organs. Under drought stress, the closure of stomata in leaves restricts photosynthetic capacity, resulting in a decrease in the efficiency of assimilate production (Tang et al., 2017; Wang et al., 2019). Additionally, after the jointing stage, there is competition between nutrient organs and reproductive organs, and the ability of different organs to compete for assimilates in response to environmental factors also plays a role in determining the fate of floret development. (Smith and Stitt, 2007; Yang et al., 2023). According to Liu et al. (2020, 2022) and Gao et al. (2023), it has been observed in corn that when resources are limited, allocating more assimilates to the spike can help reduce the loss of grain number caused by drought. The allocation of assimilates among organs under drought stress is influenced by the tolerance of the plant organs to drought (Inoue et al., 2004; Ji et al., 2010; He et al., 2022). However, the relationship between floret development and grain number formation in spikes, as well as the differential ability of spikes and stems to compete for assimilates in wheat plants with varying levels of drought resistance, still needs to be further investigated.

Assimilates accumulate in crops mainly in the form of carbohydrates, which consist mainly of sucrose, fructans, fructose, glucose, and starch (Scofield et al., 2009; Ayre, 2011; Hou et al., 2018). Sucrose, hexose and starch in the spike are the main assimilates involved in the developmental state of the spike (Clement and Audran, 1995; Dreccer et al., 2014). There is a slightly controversial view on the changes in sugar content in young spikes after experiencing drought stress (Ji et al., 2010; Zhang et al., 2020). However, there is no doubt that the process of sucrose utilization in the young spike directly determines floret development, whether under normal or adverse conditions such as drought (Shen et al., 2020), low temperature (Liang et al., 2021), high temperature (Santiago and Sharkey, 2019), and low light (Yang et al., 2023). Invertase is responsible for the irreversible decomposition of sucrose into hexose (Jiang et al., 2020). Wang and Ruan (2012) observed that in cotton, reduced expression of *GhVIN* in the seed coat is the main cause of impaired female fertility. Meanwhile, the impaired activities of ADP glucose prophorphase (AGP) and soluble starch synthase (SS) are the main reasons for the decrease in starch content in drought-stressed anthers, which in turn leads to the reduction in pollen fertility under water deficit conditions (Hu et al., 2020). However, the ability to utilize sucrose in young spikes under drought stress was also affected by the amount of assimilates transported from the stem to the spike. Fructan is the main storage form of soluble carbohydrates in wheat stems (Livingston et al., 2009; Xue et al., 2011), and it also participates in stress responses as a buffer substance (Van den Ende, 2013; Peshev and Van den Ende, 2014). The fructan contents and synthase activities (SST, FEH, FFT, etc.) in stems have an impact on both plant drought tolerance and the efficiency of carbohydrate reactivation in stems (Khoshro et al., 2014; Zhang et al., 2015a, 2015b). Sucrose is the main form of carbon assimilate transported from stems to spikes (Greco et al., 2012), and it is loaded into the phloem and unloaded into sinks (pollen, pistils, grains, etc.) by sucrose transporters (*SUTs*), and sugar will eventually be exported transporters (*SWEETs*) (Shen et al., 2023). During water shortage, the *SUT1* gene is up-regulated and expressed in monocotyledonous plants such as maize, rice, wheat and barley to maintain sucrose transport in the phloem (Lemoine et al., 2013; Kaur et al., 2021; Durand et al., 2016). However, the pattern of *SWEET* gene expression in wheat under drought is different, with most of them being up-regulated to assist anther and pollen development (Qin et al., 2020; Mathan et al., 2021; Gautam et al., 2022). In addition, sucrose is transported to the sink and absorbed into recipient cells under the action of cell wall invertase (CWINV) and sugar transporter protein (*STP*) (Ruan, 2014; Wang and Ruan, 2012). Previous studies have shown that *STP* is involved in seed and pollen development (Rottmann et al., 2018) and is involved in the physiological response of plants to drought stress (Bavnhoj et al., 2021). Therefore, exploring the mechanisms of drought-induced differences in sugar utilization by young spikes as well as stem-to-spike translocation of sugars in different drought-resistant wheat varieties is essential to explain the differences in the number of grains.

We conducted a field shelter experiment over two winter wheat growing seasons using ^{13}C isotope labelling to quantify assimilate partitioning between organs and further combined it with physiology and transcriptomics to investigate key differences in assimilate transport between organs and sucrose and starch metabolism in response to drought stress and their relationship with floret development and grain number in spikes. Therefore, we hypothesized that (1) the transport of assimilates in various organs of wheat is linearly related to the degradation of florets under drought conditions; (2) wheat with strong drought resistance has a stronger ability to utilize sucrose in young spikes and an advantageous ability to transport assimilates from stem to spike; and (3) dominant spike-stem competition for assimilates contributes to spike grain number under drought stress.

2. Materials and methods

2.1. Experimental design

Experiment I: The experiment was conducted during 2020–2022 at a rain shelter (78 m × 18 m) in the Yangling Smart Agriculture Valley in the Yangling Demonstration Area, Shaanxi Province, China (34°15′N, 108°02′E). The daily average temperature during the growth period of winter wheat was shown in Li et al. (2023). Winter wheat (*Triticum aestivum* L.) cultivars Changhan58 (CH58, strong drought resistance) and Luohan6 (LH6, weak drought resistance) were selected. The winter wheat was sown on October 25 and 20, 2020 and 2021, with a seeding rate of 165 kg ha $^{-1}$ and a row spacing of 25 cm. Three soil water gradient treatments were set in the experiment: well-watered condition (WW) treatment (soil relative humidity 70–75%), moderate soil drying (MD) treatment (soil relative humidity 60–65%) and severe soil drying (SD) treatment (soil relative humidity 50–55%). The two water-deficit treatments started at the jointing stage (S1, Feekes8, Feekes, 1941) and lasted until the heading stage (S3, Feekes10.5). A two-factor randomized block design with cultivar and soil water treatment was adopted in the experiment. The specific details of soil water control as described by Li et al. (2023). The relative soil water content during the three critical periods is shown in Fig. 1. The plots were all restored back to the control level after the heading stage. The initial soil nutrients of the upper soil layer (0–20 cm) at the beginning of the experiment are shown in Table S1.

Experiment II: The chemical application experiment was conducted at the above experimental site in the 2021–2022 growing season. As described by Li et al. (2023), three experimental treatments were established: WW + water spray (WW); several drought stress + water spray (DS); and several drought stress + spermidine spray (DS-Spd). The area of each plot was 6 m^2 (2 m × 3 m) at an interval of 2 m. The experimental cultivars and soil watering regime are the same as in Experiment I. Water and chemical solutions were carefully sprayed from 16:00 to 18:00 for 2 consecutive days, starting 5 days before the booting stage (S2, flag leaf pillow pulled out 4–6 cm).

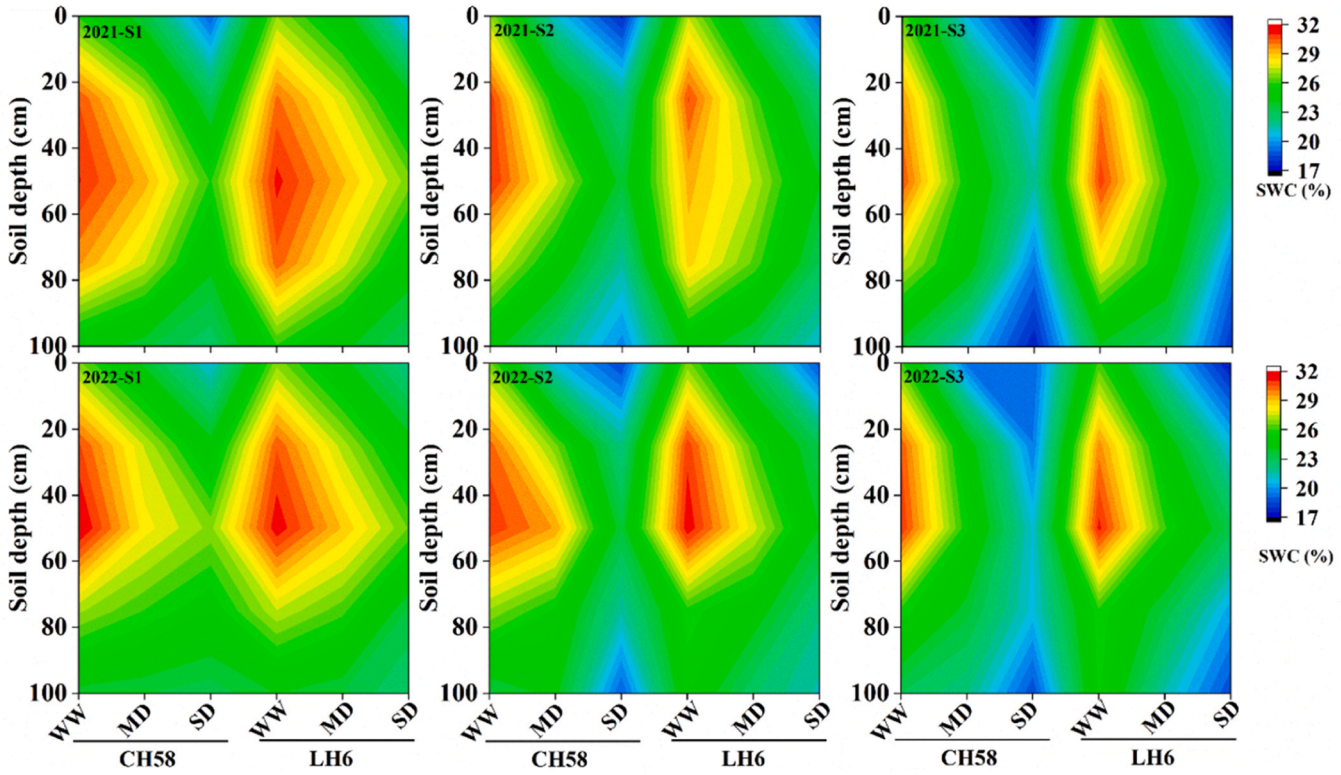

Fig. 1. Soil volumetric water content in the 0–100 cm soil layer at the jointing-heading stage. SWC (%) means relative soil water content (%). S1: the jointing stage (Feekes8) (the flag leaf tip was 2–4 cm); S2: the booting stage (Feekes9) (the wheat flag leaf pillow emerged 4–6 cm); and S3 (Feekes10.5): the heading stage (the spike of wheat emerged 4–6 cm).

2.2. Soil water storage and consumption

The 1 m long TDR tubes were buried vertically between the wheat rows of each plot, and an AZS-100 TDR sensor was used to determine the soil water content in situ. Measurements were taken every three days from jointing to heading and every 1–2 weeks at other times at 20 cm intervals to a depth of 100 cm. The soil water storage (SWS) (mm) for each layer was determined according to the following equation:

$$SWS=\sum SWCi\times SDi\times 10/100 \quad (1)$$

where SWS is the soil water storage of soil layer i (mm), SWCi is the volumetric soil water content (%) in soil layer i, and SDi is the depth of soil layer i (cm).

Water consumption in all treatments was estimated by calculating the water balance in the 0–100 cm soil layer:

$$\text{Water consumption (mm)} = I+\Delta SWS + P - R - D \quad (2)$$

where I is the irrigation (mm), ΔSWS is the decrease in soil water stored in the 0–100 cm soil layer from jointing to heading (mm), P is the precipitation (mm), which could be disregarded because the experimental site had a rain shelter to avoid rainfall during the whole growth period, R is the runoff (mm), D is the deep penetration, and R and D could be disregarded because the experimental site is flat and the underground water level is deep.

2.3. Plant sampling and measurements

2.3.1. Development of wheat florets

The process of spike differentiation was observed and recorded by an XTS2022 electron optical microscope (Beijing Tech). At the jointing stage (S1, Feekes8, flag leaf of wheat was exposed for 2–4 cm) and heading stage (S3, Feekes10.5, the spike of wheat was pulled out for 4–6 cm), fifteen main stems with consistent development were taken to observe and record the maximum differentiation number of florets and the number of fertile florets at each flower position at different spikelet positions (the florets with complete green anthers and pinnate stigmas as the judgment standard of fertile florets). At maturity, fifteen spikes were sampled to determine the grain number per spike. Three replicates were performed for each plot.

2.3.2. Relative water content (RWC), photosynthetic parameters and relative chlorophyll content (SPAD value)

RWC (%) was determined using the Hunt et al. (1987) method. At the booting stage, six flag leaves were selected from each plot, and their fresh weight was recorded. Samples were then dipped in a plastic box filled with water and kept for 24 h. After 24 h, the samples were removed, and the turgor weight was recorded. Next, these leaves were kept in an oven at 75 °C for 72 h, and the dry weight was recorded. The RWC was calculated by the following formula:

$$RWC=(FW-DW)/(TW-DW)\times 100 \quad (3)$$

where FW is fresh weight (g), DW is dry weight (g), and TW is turgor weight (g).

The photosynthetic parameters, including net photosynthesis rate (Pn), stomatal conductance (Gs), and transpiration rate (Tr), were determined for the flag leaves using a Li-6400XT system (Li-COR, USA) at the booting stage of winter wheat (April 1 and 5 from 2021 to 2022, respectively) during 9:00–11:30 am on sunny days, and six leaves were selected at random to measure for each treatment. The light intensity and flow rate were maintained at 1100 μmol·m^{-2}·s^{-1} and 500 mL min^{-1}, respectively. The ambient CO_2 concentration was measured to be 400 μmol mol^{-1}. The instantaneous water use efficiency (WUEi) of leaves was calculated as follows (Ou et al., 2015):

$$WUEi=Pn/Tr \quad (4)$$

where WUEi (μmmol $mmol^{-1}$) is the instantaneous water use efficiency of leaves, Pn (μmol m^{-2} s^{-1}) is the net photosynthetic rate, and Tr (mmol m^{-2} s^{-1}) is the transpiration rate.

The SPAD values were determined for the flag leaves using a SPAD 502 Plus system (Konica Minolta, Japan) at the booting stage in winter wheat (March 30 and April 5 from 2021 to 2022, respectively) during 9:00–11:00 am on sunny days. Nine leaves were selected at random for each treatment.

2.3.3. Lipid peroxidation and antioxidant enzymes

The malondialdehyde (MDA) content was measured as a product of lipid peroxidation using thiobarbituric acid (TBA) according to Hodges et al. (1999). Fresh leaves (0.15 g) were ground with 5.0 mL of 5% (w/v) trichloroacetic acid (TCA) in a mortar that was placed in an ice bath, and then the supernatant fluid was collected after centrifugation for the MDA assay. MDA content was measured by a spectrophotometer at 600 nm and 532 nm. As described by Jiang and Zhang (2002), superoxide dismutase (SOD; EC 1.15.1.1) activity was assayed by monitoring the inhibition of photochemical reduction of nitro blue tetrazolium (NBT) at 550 nm, and catalase (CAT; EC 1.11.1.6) activity was assayed by measuring the disappearance of H_2O_2 at 240 nm. The method of Maehly and Chance (1955) was used to determine the peroxidase (POD) activity, in which guaiacol was converted to tetraguaiacol, which was monitored at 470 nm (Jiang et al., 2020). Ascorbate peroxidase (APX; EC 1.11.1.11) activity was determined by the decrease in absorbance at 290 nm following the method of Sharma and Dubey (2004).

2.3.4. Assimilate accumulation and distribution, $^{13}CO_2$ labelling, sampling and calculations

At the jointing, booting and heading stages, fifteen representative plants were harvested from each plot. Each plant was divided into spike, leaf, stem, and sheath sections, dried at 105 ℃ for half an hour, and then dried at 75 ℃ to a constant weight.

The labelling principle is to use HCl (1 mol L^{-1}) and $Na_2^{13}CO_3$ (99 atom% ^{13}C, Sigma—Aldrich) to react to generate $^{13}CO_2$ gas so that the concentration of CO_2 gas in the labelling room reaches 500 μL L^{-1}. The CO_2 analyser, four 50 mL centrifuge tubes with the same amount of $Na_2^{13}CO_3$ and an empty beaker (50 mL) were placed into the labelling room before isotopic labelling, and then the bottom of the chamber was sealed with water. The labelling room was a transparent PVC box (0.4 m × 0.4 m × 0.7 m, l×w×h) fitted with a circulating fan at the top (Fig. S1). It started at 8:00 on a sunny morning (March 20 (LH6) and March 22 (CH458) in 2021, jointing stage) using an infrared CO_2 analyser to monitor the CO_2 concentration in the labelling room (Wu et al., 2009). When it dropped to 80 μL L^{-1}, HCl (1 mol L^{-1}, 10 mL) was added to one of the centrifuge tubes containing $Na_2^{13}CO_3$. Then, the fan was turned on, and the newly generated $^{13}CO_2$ in the room was evenly distributed. When the CO_2 concentration in the labelling room dropped again to 80 μL L^{-1} (approximately 15 min), the same amount of HCl was added to the second centrifuge tube. The same steps were performed for the third and fourth beakers containing $Na_2^{13}CO_3$, and the same amount of HCl was added. After adding HCl for the fourth time for 15 min, NaOH solution was added to the empty beaker to absorb the remaining $^{13}CO_2$ in the room and reduce the diffusion loss of $^{13}CO_2$ into the air. At the end, the marking chamber was moved away when the CO_2 concentration dropped below 80 μL L^{-1}, and the whole marking process was over.

After isotope labelling for 6 h (S1-AL6h) and 8 days (boot stage, S2-AL8d), 15 individual plants were selected for each treatment and divided into leaves, stems, sheaths, and spikes. The wheat tissues were oven dried at 85 °C for 3 h and then dried at 65 °C until a constant weight was reached for mass measurements. The dried samples were ground to pass through a 0.149-mm sieve for subsequent analyses. The total C contents and $\delta^{13}C$ values of plants were measured by using an elemental analyser (Elementar Vario PYRO cube, Germany) coupled with an isotope ratio mass spectrometer (IsoPrime 100 isotope ratio mass spectrometer, Isoprime100, Germany). The results of the C isotope analyses are expressed in δ units as follows:

$$\delta^{13}C\ (‰) = [(Rsample/Rstandard) - 1] \times 10^3 \quad (5)$$

where R is the ratio of $^{13}C/^{12}C$ for both samples (Rsample) and standards (Rstandard). The $\delta^{13}C$ of all tissues is shown in Fig. S2.

The photosynthesized C (mg) in wheat was represented by the product of the C content percentage (%) and dry matter weight (mg). The content of ^{13}C-photosynthates of each tissue in wheat was calculated as follows (Liu et al., 2020):

$$^{13}C\text{-photosynthates}_{(i)}\ (mg) = \text{photosynthesized}\ C_{(i)} \times (\delta 13C_{t(i)} - \delta^{13}C_{0(i)}) \quad (6)$$

where i represents each wheat tissue, including the young spikes, leaves, stems and sheaths; $\delta^{13}C_{0(i)}$ and $\delta^{13}C_{t(i)}$ (‰) represent the $\delta^{13}C$ of each wheat tissue i of ^{13}C unlabelled and labelled, respectively.

The distribution rate of ^{13}C-photosynthates (%) was calculated by the percentage of ^{13}C-photosynthates of each tissue in the ^{13}C-photosynthates of the whole plant (Zhao et al., 2021). The transport rate of ^{13}C-photosynthates (^{13}C-photosynthates TR) from the S1 to S2 period was calculated as follows:

$$^{13}C\text{-photosynthates TR}_{(i)}\ (\%) = (^{13}C\text{-photosynthates 2}_{(i)} - {}^{13}C\text{-photosynthates 1}_{(i)})/{}^{13}C\text{-photosynthates 2}_{(i)} \times 100 \quad (7)$$

where i represents the same as formula (7); ^{13}C-photosynthates 2 represent the ^{13}C-photosynthates $_{(i)}$ (mg) of S2, and ^{13}C-photosynthates 1 represent the ^{13}C-photosynthates $_{(i)}$ (mg) of S1.

2.3.5. Concentrations of glucose, sucrose, fructose, fructan and starch

The dried samples were ground into powder and sieved (0.5 mm aperture) for sugar and starch measurement. Sugars were extracted according to Wardlaw and Willenbrink (1994) with slight modifications. In brief, 100 mg tissue samples were extracted directly in 5 mL alcohol (90%, v/v) in an 80 ℃ water bath for 10 min, the supernatant was collected, and the residues were extracted a second time by the same method. The supernatant was merged and evaporated in a 90 ℃ water bath until dryness. It was dissolved thoroughly in 1 of distilled water and then passed through a 0.45 μm filter membrane. Ten microliters of extractives was used to quantify glucose, fructose, and sucrose concentrations by HPLC (Agilent 1260, Agilent Technologies, Santa Clara, USA). The HPLC column was a ZORBAX Carbohydrate column (4.6 × 150 mm, 5 μm), the column temperature was 35 ℃, the mobile phase system was an acetonitrile:water mixture (80:20, v/v), and the flow rate was 1 mL min^{-1}. According to Hanft and Jones (1986) with slight modifications, the WSC and starch concentrations were obtained via the anthrone method. The total fructan concentration was calculated as the total WSC minus the glucose, fructose, and sucrose (Zhang et al., 2015a, 2015b).

2.3.6. Activities of invertase, 1-fructan exohydrolase, and sucrose:sucrose 1-fructosyltransferase

The extract of soluble vacuolar invertase (INV) and cell wall invertase (CWIN) was reported by Zinselmeier et al. (1999). Enzyme activities were determined using a spectrophotometer, according to Shen et al. (2018). Frozen tissue samples (0.1 g) were ground to a fine powder in liquid nitrogen and then homogenized in extraction buffer (pH 7.4 PBS buffer, 0.9 mL). The extracts were centrifuged at 8000 rpm for 30 min at 4 °C, and the supernatant was used for determination of 1-fructan exohydrolase (1-FEH) and sucrose: sucrose 1-fructosyl-transferase (1-SST) activities. 1-FEH and 1-SST activities were measured using ELISA kits from Ruixin Biotechnology Co., Ltd. (Quanzhou, China).

2.3.7. RNA extraction, transcriptome sequencing and differential gene expression analysis

After sampling, the samples of S2 (peak period of floret degeneration, Feekes9) were immediately stored in liquid nitrogen and placed at −80 ℃ for RNA extraction and sequencing. Total RNA was extracted

from the spike and root samples using an E.Z.N.A. plant RNA kit (Omega Bio-Tek, USA) following the manufacturer's instructions. Only high-quality RNA samples (OD260/OD280 was 1.9–2.0) were used for library construction. Sequencing libraries were constructed according to the manufacturer's protocol of Illumina's NEBNext Ultra II RNA Library Prep Kit (NEB, Ipswich, USA). Subsequently, the libraries were sequenced using an Illumina HiSeq 2500 platform by BioMarker Technologies Inc. (Beijing, China).

After removing adaptor sequences and filtering low-quality sequences, clean reads from each sample were mapped to the reference genome of IWGSC_RefSeq_v1.1 (https://urgi.versailles.inra.fr/download/iwgsc/IWGSC_RefSeq_Annotations/v1.1/) by HISAT2. The expression of each gene was normalized to fragments per kilobase of transcript per million reads (FPKM) to compare among different samples. DESeq2 was adopted to estimate the differential gene expression between SD and CK. Genes with a p value ≤ 0.01 and a fold change ≥ 1.5 were defined as differentially expressed genes (DEGs). Functional enrichment analyses of DEGs were performed using KEGG. As TPM values are more suitable for comparison between samples, we analysed the genes encoding sucrose and starch metabolism enzymes by converting FPKM values to TPM values using the following formula (Li et al., 2010):

$$\mathrm{TPM} = \left(\frac{\mathrm{FPKM}}{\sum \text{all genes FPKM}}\right) \times 10^6 \quad (8)$$

Quantitative real-time PCR (qRT–PCR) analysis was performed to test the results of RNA-seq of nine selected genes using RNA extracted from independently grown and treated wheat.

2.3.8. Observation of vascular bundles in wheat nodes

In S2 during the 2022 growth season, the fresh stem (the second internode below the spike) was used to observe vascular bundles. The fresh materials were removed, immediately placed in the fixing solution and stored overnight at 4 ℃. The conventional paraffin sectioning method was used for embedding materials and continuous sectioning, with a thickness of 10 μM. The slices were double stained with saffron and solid green. Slices were imaged using stereomicroscopy (SZX16, Olympus, Japan). The graphics software ImageJ was used to measure the vascular bundle areas. Three to four technical replicates were performed for each biological replicate.

2.3.9. Content of endogenous spermidine

Spermidine was extracted and measured according to the methods of Liu et al. (2016). Briefly, 0.5 g of fresh sample was ground into homogenate with 3 mL of precooled 5% (v/v) perchloric acid (PCA) in a precooling mortar. The supernatant was derivatized with benzoyl chloride and used for determination. 10 μL of extract was quantified by HPLC (Agilent 1260, Agilent Technologies, Santa Clara, USA).

2.4. Statistical analysis and graphing

SPSS 26 software (SPSS Inc., Chicago, IL, USA) was used to analyse significance. Three-way ANOVA with year, cultivar and treatment as fixed factors were conducted to determine the significance of treatment effects. Differences between means were compared by a least significant difference (LSD) test at a P value < 0.05. Linear fitting was used to describe the relationship between the floret degeneration rate and the transportation ratio of ^{13}C-photosynthate grains. Figures were completed using Origin 2022, R language (version 3.6.1, RStudio, Boston, USA), Adobe Illustrator (version CS6, Adobe, San Jose, USA), and Microsoft PowerPoint 2016 (Microsoft, Redmond, USA).

3. Results

3.1. Soil water storage and consumption, floret development and setting characteristics

In the 0–100 cm soil layer, the 20–80 cm soil layer had higher water storage (Fig. 2A). With the progress of wheat growth, compared with WW, the soil water storage of MD and SD showed a decreasing trend. Under MD and SD conditions, soil water storage in the 0–100 cm soil layer from S1 to S3 decreased by an average of 12.6–15.7% (CH58) and 10.0–16.5% (LH6), respectively. Drought significantly suppressed the water consumption of wheat in the S2-S3 stage, but there was no significant difference in water consumption between the two cultivars (Fig. 2B).

The cultivar, soil moisture and their interaction significantly affected the number of fertile florets, floret degradation rate and grain number per spike (Table 1). The number of fertile florets and grains per spike showed highly significant positive correlations with soil water content, while the rate of floret degradation and abortion showed highly significant negative correlations with soil water content, respectively (Fig. S3). Under the conditions of MD and SD, the number of grains was significantly reduced by 7.9%−21.0% in 2021 and 4.9%−15.7% in 2022 compared to CK for CH58 and reduced by 17.7%−32.4% in 2021 and 12.9%−20.9% in 2022 for LH6. Further analysis of the change in floret number showed that drought stress (MD and SD) did not significantly affect the maximum number of florets in the two growing seasons but significantly decreased the number of fertile florets by 5.2%−16.5% in 2021 and 4.2%−8.6% in 2022 compared to CK for CH58 and reduced it by 11.4%−26.4% in 2021 and 8.7%−14.5% in 2022 for LH6, thus significantly increasing the average rate of floret degradation by 2.1%−4.2% (CH58) and 2.9%−7.1% (LH6). In addition, the abortion rate was significantly reduced by 1.4%−5.8% (CH58) and 5.0%−6.5% (LH6) under MD and SD treatment. In general, soil drought stress had more severe effects on floret development and seed setting in LH6.

3.2. Photosynthesis of leaves and antioxidant capacity of young spikes and leaves

In the 2020–2022 growing seasons, drought stress (MD and SD) significantly reduced the relative water content (RWC) and relative chlorophyll content (SPAD) of flag leaves at the booting stage compared to WW, and the decline increased with the intensification of drought (Fig. 3). At the same time, compared with WW, SD significantly reduced the net photosynthetic rate (Pn) by 15.7–48.2% (CH58) and 25.0–30.3% (LH6), transpiration rate (Tr) by 11.7–17.2% (CH58) and 15.7–17.1% (LH6), stomatal conductance (Gs) by 42.4–48.2% (CH58) and 38.2–54.9% (LH6), and instantaneous water use efficiency (WUEi) of leaves by 1.5%−4.7% (CH58) and 10.9%−16.0% (LH6). The Pn, Gs, Tr, RWC and SPAD of flag leaves were significantly and positively correlated with the number of fertile florets and the number of grains per spike (Fig. S4). The degradation rate of fertile florets was significantly negatively correlated with the Pn, Gs, RWC, and SPAD of flag leaves.

In comparison to WW, drought (MD and SD) stress significantly increased malondialdehyde (MDA) content (especially from S2) and ascorbate peroxidase (APX) and catalase (CAT) activities, while the content of soluble protein (except LH6) was reduced in spikes (Fig. 4). Among them, the increase in MDA and APX in the spike of CH58 was higher than that of LH6. With increasing drought (from S1 to S3), superoxide dismutase (SOD) and peroxidase (POD) activities in the spikes of both cultivars first increased and then decreased. For leaves, drought significantly increased MDA content (higher for LH6 than for CH58) when soluble protein, SOD, POD, CAT, and APX were significantly inhibited. Therefore, the antioxidant capacity of the spike gradually weakened, and the degree of leaf peroxidation was higher (LH6 was more pronounced) as drought intensified.

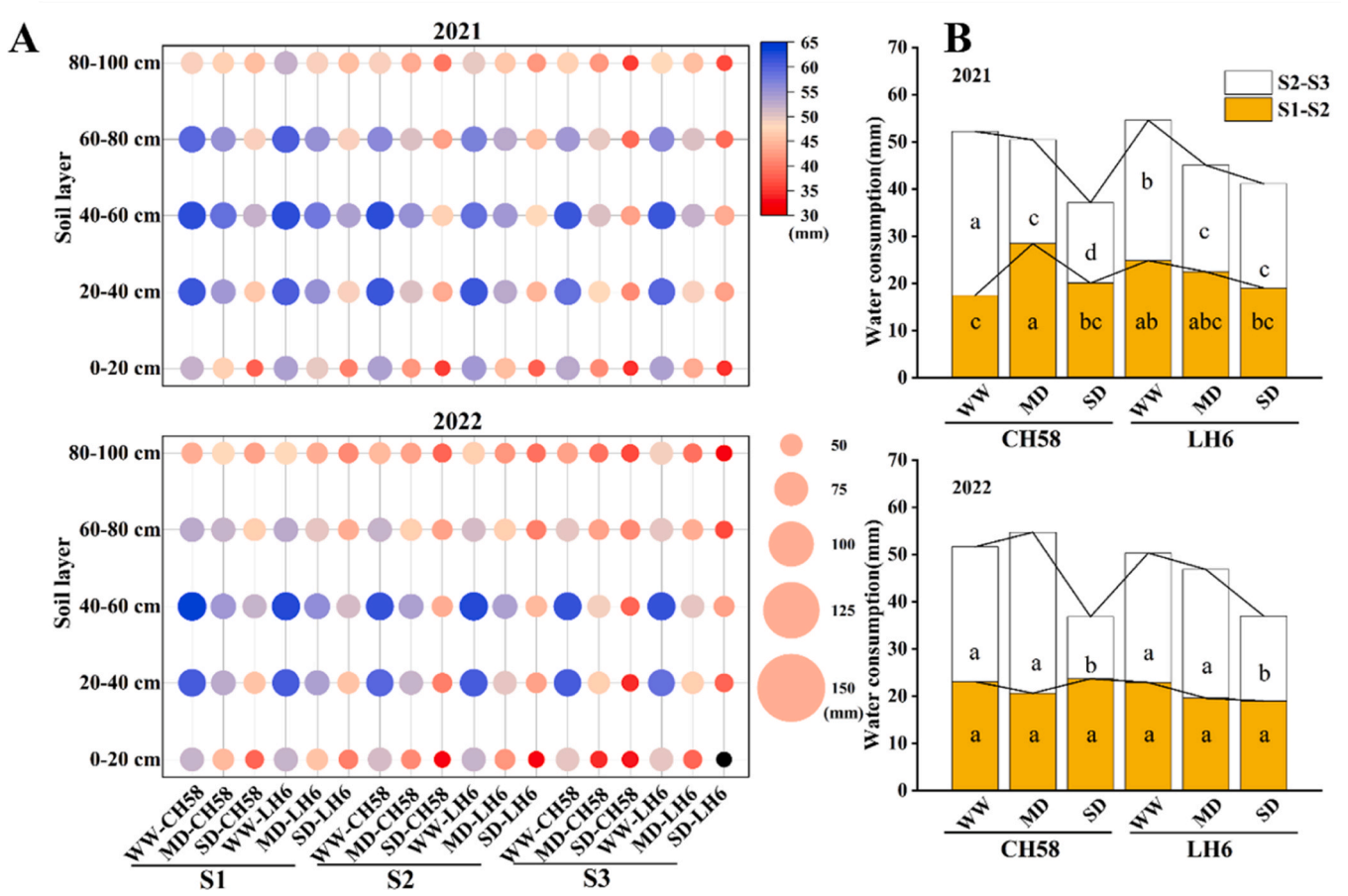

Fig. 2. Soil water storage (A) and wheat water consumption (B) in the 0–100 cm soil layer. S1: the jointing stage (Feekes8) (the flag leaf tip was 2–4 cm); S2: the booting stage (Feekes9) (the wheat flag leaf pillow emerged 4–6 cm); and S3 (Feekes10.5): the heading stage (the spike of wheat emerged 4–6 cm).

Table 1
Wheat floret development and grain set characteristics during the 2020–2021 and 2021–2022 growing seasons.

Years	Cultivars	Treatments	Maximum number of floret differentiation	fertile florets	Floret degradation rate (%)	Grains number	Abortion rate (%)
2020-2021	CH58	WW	146a	50.2b	65.6c	41.6b	17.2b
		MD	153a	47.6c	68.9b	38.3c	19.4 ab
		SD	154a	42.0d	72.7a	32.9d	21.6a
	LH6	WW	150a	53.5a	64.3c	44. 7a	16.5b
		MD	151a	47.4c	68.6b	36.8c	22.4a
		SD	153a	39.4e	74.3a	30.2d	23.2a
2021-2022	CH58	WW	154a	50.4a	67.6d	46.7a	7.4c
		MD	153a	48.3b	68.5cd	44.4a	8.0c
		SD	148a	46.1c	69.0c	39.3b	13.0a
	LH6	WW	155a	48.2b	69.0c	41.0a	14.9c
		MD	150a	44.0d	71.6ab	35.7b	18.9ab
		SD	154a	41.2e	73.3a	32.4d	21.2a
ANOVA	Year (Y)		ns	ns	ns	* *	* *
	Treatment (T)		ns	* *	* *	* *	* *
	Cultivar (C)		ns	* *	* *	* *	* *
	Y×C		ns	* *	* *	* *	* *
	Y×T		ns	* *	* *	*	ns
	C×T		ns	**	*	*	ns
	Y×C×T		ns	ns	ns	ns	ns

Note: WW, MD and SD represent well-water condition (as the control group), moderate drought and severe drought stress treatment, respectively, from booting to heading stage. Data were from two study years (2020-2021 and 2021-2022). Different lowercase letters denote significant differences at 0.05 levels. * and * * indicate significance at the $P < 0.05$ and 0.01 levels, respectively; ns, no significant difference.

3.3. Accumulation and distribution of assimilation and ^{13}C enrichment in wheat tissues

At the S2 stage, the SD treatment significantly reduced the dry matter accumulation of the whole wheat plant, while moderate drought had no significant inhibition trend, especially for LH6 (Fig. 5A). Further utilizing ^{13}C labelling to quantify assimilate allocation, the results showed that the abundance of ^{13}C in labelled young spikes was the highest (Fig. S2). SD significantly reduced the ^{13}C-photosynthates of young spikes at the booting stage (S2) by 15.7% (CH58) and 24.7% (LH6), as

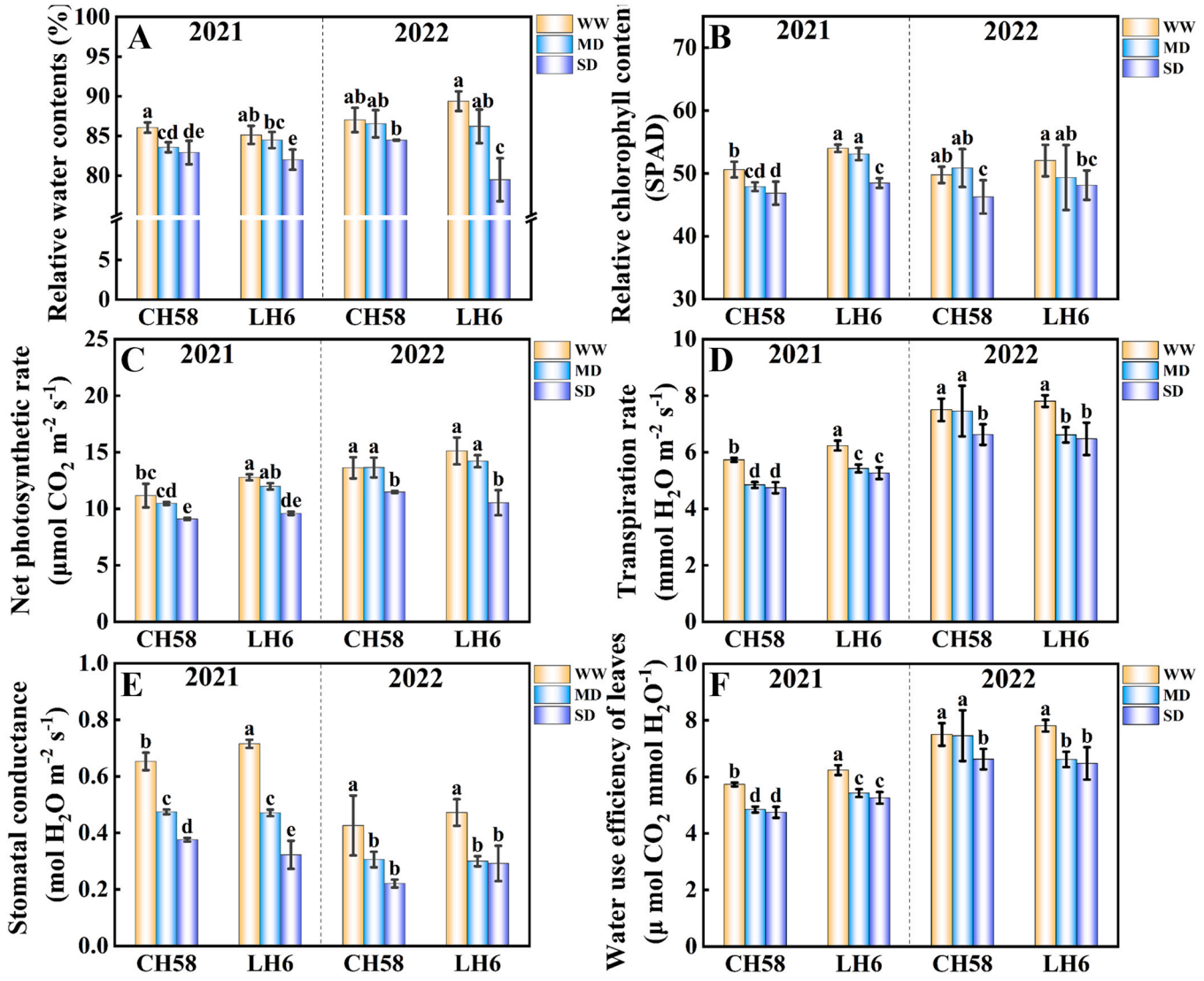

Fig. 3. Leaf water status, chlorophyll content and photosynthetic parameters of flag leaves under different treatments. (A) Relative water content; (B) Relative chlorophyll content (SPAD); (C) Net photosynthetic rate (Pn); (D) Transpiration rate (Tr); (E) Stomatal conductance (Gs); (F) Water use efficiency (WUEi). The data for A-F were from S2 (Feekes9) of the 2020–2021 and 2021–2022 growing seasons. Values are means ± SD (n = 3). Different lowercase letters denote significant differences (ANOVA, Fisher's least significant difference test, $P < 0.05$).

well as the ^{13}C-photosynthates of leaves of CH58 and LH6 by 9.7% and 33.4%, respectively, compared with WW (Fig. 5B). In the S1 and S2 stages, 63.2%−70.0% of the ^{13}C-photosynthates were allocated to stems and sheaths (Fig. 5C). During the S2 period, compared with WW, SD significantly reduced the ^{13}C photosynthetic carbon content of the stem by 8.5% (CH58) and 11.7% (LH6), as well as the ^{13}C photosynthetic carbon content of the sheath of CH58 and LH6 by 18.3% and 13.2%, respectively (Fig. 5B).

We further analysed the transportation ratio of ^{13}C-photosynthates from the S1 to S2 stages and found that 42.5%−59.3% of ^{13}C-photosynthates in young spikes were transported from other organs, and drought stress played an inhibitory role in this process (Table 2). Under drought conditions, ^{13}C-photosynthates translocated to young spikes originating from leaves, stems, and sheaths for LH6 but only from stems for CH58. Therefore, there are significant differences in the allocation strategies of assimilates between the two cultivars under drought conditions. Linear fitting was performed on the ^{13}C allocation ratio and floret degradation rate of each organ in the two cultivars, and the results showed that the ^{13}C allocation rate of the stems of CH58 was positively correlated with the floret degradation rate, with a coefficient of $R^2 = 0.77$, while that of LH6 was negatively correlated, with a coefficient of $R^2 = 0.74$ (Fig. 5D).

3.4. Differentially expressed genes in spike and stem

To understand the different responses of young spikes and stems of the two genotypes to drought, we conducted four pairwise comparisons of stems and spikes of CH58 and LH6 between well-watered (WW) and severe drought (SD) treatments (Fig. 6). A total of 396 (232 genes were upregulated and 164 were downregulated) differentially expressed genes (DEGs) were identified in spikes and 459 (334 genes were upregulated and 125 were downregulated) DEGs in stems (DEG threshold: P value <0.01 and fold change ≥1.5) of CH58 under SD treatment compared to WW (Fig. 6A). LH6 showed stronger drought-induced changes, with a total of 9886 (5512 genes were upregulated and 4374 were downregulated) DEGs in spikes and 11227 (4885 genes were upregulated and 6342 were downregulated) DEGs in stems. The reliability of the transcriptome data was determined by qRT—PCR with 9 randomly selected genes. The results showed that the trend of upregulation or downregulation of gene expression was consistent with the

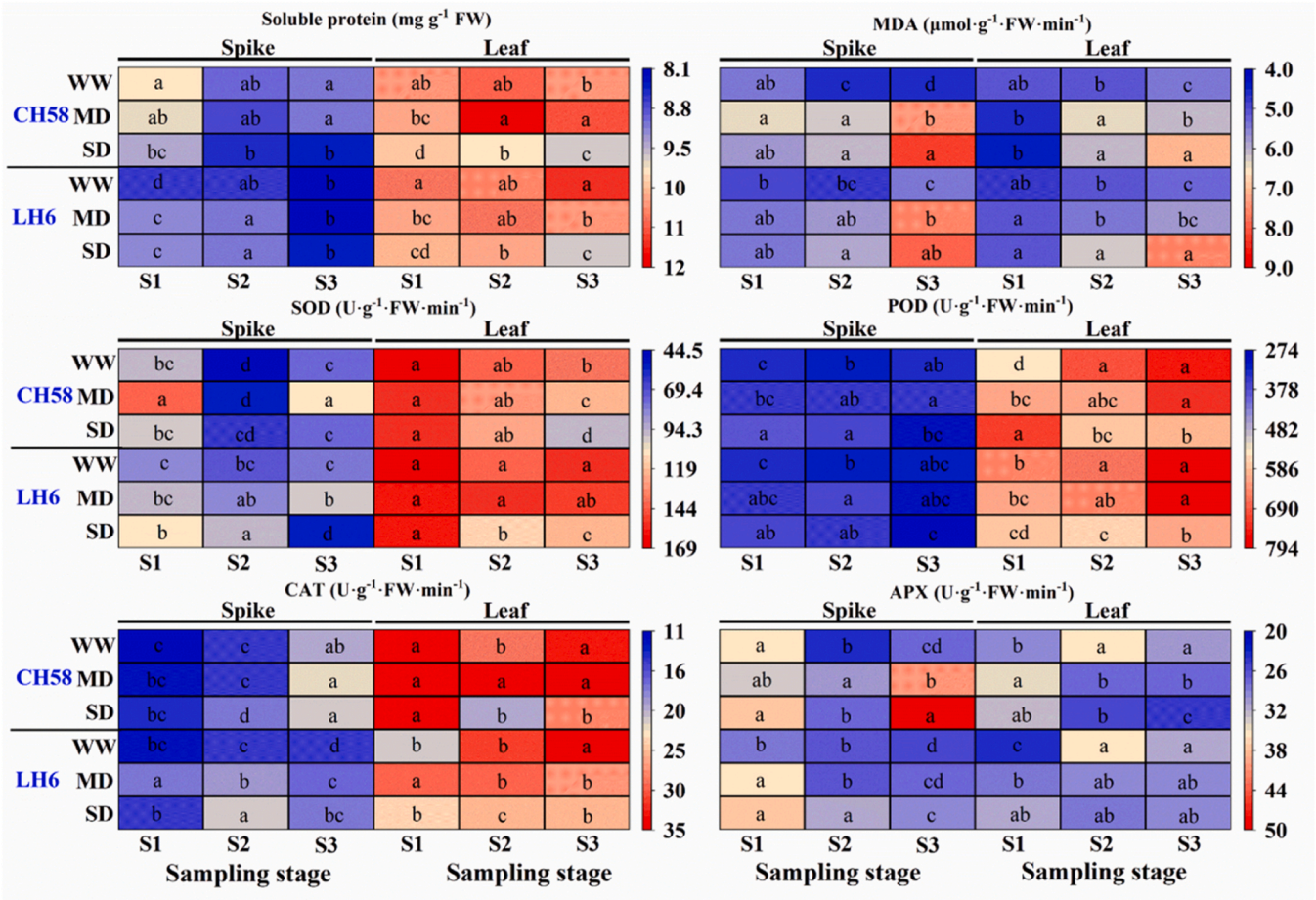

Fig. 4. Osmolyte and antioxidant activity of spikes and leaves under different treatments. (A) Soluble protein content. (B) Malondialdehyde (MDA) content. (C) Superoxide dismutase (SOD) activity. (D) Peroxidase (POD) activity. (E) Catalase (CAT) activity. (F) Ascorbate peroxidase (APX) activity. The data were from the 2021–2022 growing season. Values are means (n = 3). Different lowercase letters denote significant differences (ANOVA, Fisher's least significant difference test, $P < 0.05$).

transcriptome data (Fig. S5).

A large number of DEGs were enriched in pathways related to carbohydrate metabolism, including carbon metabolism (Ko01200), carbon fixation in photosynthetic organisms (ko00710), starch and sucrose metabolism (ko00500), glycolysis/gluconeogenesis (ko00010), and glyoxylate and dicarboxylate metabolism (ko00630) (Fig. 6B; Table S2). Significantly, there were 138 and 140 DEGs enriched in sucrose and starch metabolism pathways in the spike and stem of LH6, respectively, which were far more than those in CH58. Therefore, the number of DEGs in the spike and stem of LH6 was far greater than that of CH58, and more DEGs for LH6 were also enriched in the pathway of sucrose and starch metabolism by drought.

3.5. Concentration of sucrose, hexose, fructan, and starch in spike and stem

The contents of sucrose and hexose in young spikes and stems during the booting and heading stages were greatly affected by soil drought (Fig. 7). In young spikes, drought significantly reduced sucrose, fructose and glucose contents (Fig. 7A-C), and in S2, the decrease in fructose and glucose contents was higher in LH6 than in CH58 (especially in the 2021–2022 growing season) (Fig. S6). In the stems, MD and SD significantly increased the glucose and fructose contents (SD increased more in LH6 than in CH58), while the sucrose content decreased. Notably, the decrease in sucrose in CH58 stems was higher than that in LH6 stems. For fructan, SD treatment significantly reduced fructan in the young spikes of S2 and S3 but significantly increased it in the stems (the increase in CH58 was higher than that in LH6) (Fig. 7D). Meanwhile, drought significantly reduced the starch content in young spikes when the starch content in stems first increased and then decreased by drought, and there was no significant difference in the reduction between the two cultivars (Fig. 7E). The effect of drought on hexose, sucrose, fructan and starch in the 2021–2022 growing season was the same as that in the 2020–2021 growing season (Fig. S6). Hence, the hexose and sucrose contents in the spikes of LH6 and sucrose and fructan contents in the stems of CH58 were more responsive to drought, which was related to enzymes and genes involved in sucrose transport and metabolism.

3.6. Gene expression and enzymatic activity involved in sucrose transport and metabolism

The genes involved in sucrose transport and metabolism pathways in these young spikes and stems are shown in Fig. 8A. Compared to WW, the genes encoding sucrose synthesis-related enzymes (e.g., sucrose-phosphate synthase (*SPS*) and sucrose synthase (*SUS*)) were highly expressed in the spike and stem of CH58 under SD treatment but were downregulated in LH6. The expression of genes encoding sucrose decomposition-related enzymes such as invertase (*INV*), hexokinase (*HK*), fructokinase (*FRK*), and alpha-glucosidase (*malZ*) was increased by SD in young spikes of CH58. *INV* and *HK* were highly expressed under drought in the stems of CH58, while *FRK* and *malZ* were downregulated. The above genes related to sucrose decomposition (except *HK*) were suppressed in the young spike of LH6 and were upregulated in the stem

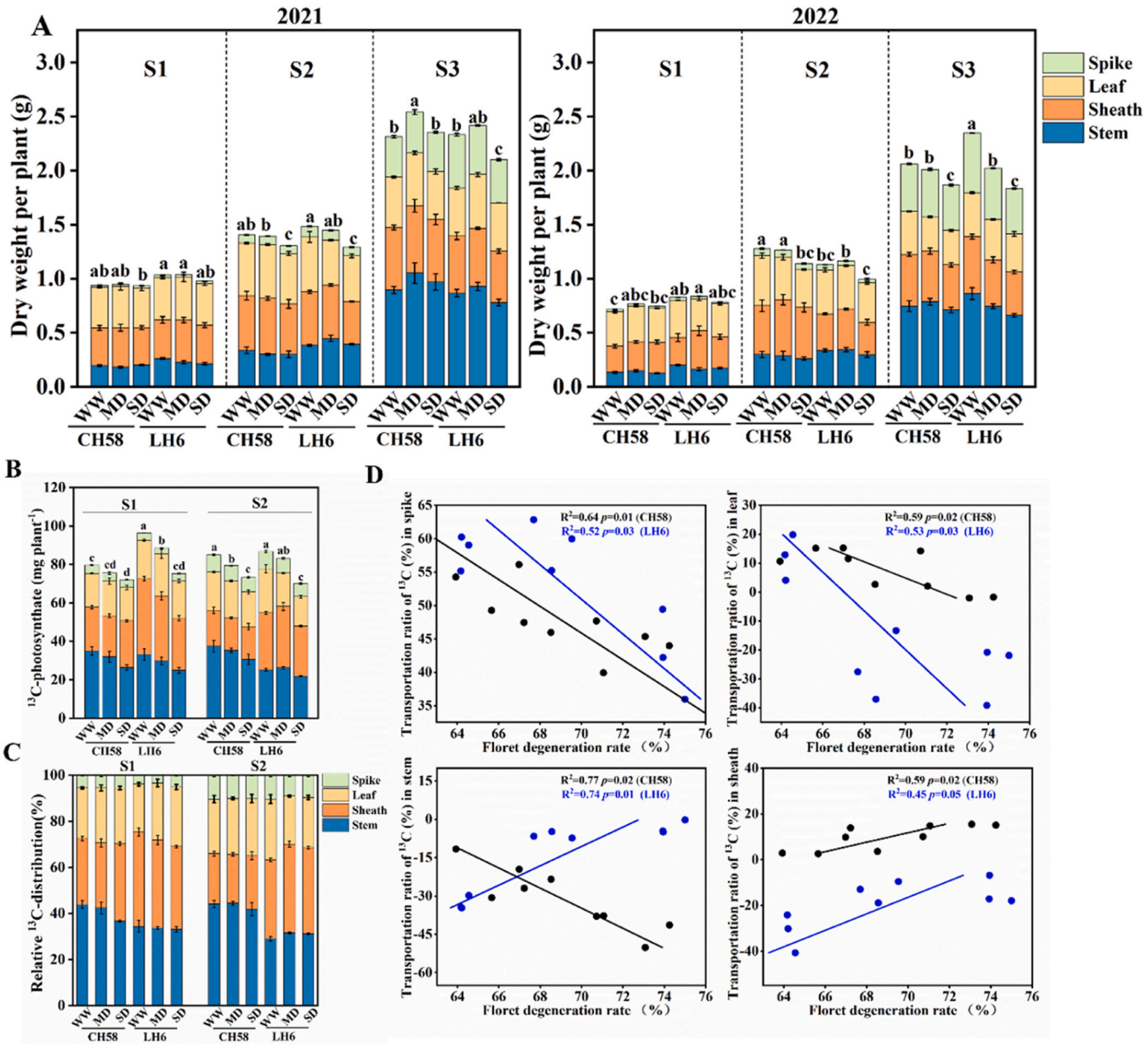

Fig. 5. Accumulation and distribution of dry matter (A) and ^{13}C-photosynthates (B-C) in wheat organs and the linear relationship between the floret degradation rate and translocation rate of ^{13}C-photosynthates (D). S1: the jointing stage (Feekes8) (after labelling for 6 h); S2: the booting stage (Feekes9) (after labelling for 8 days). The data for B-D were from S1 (Feekes8) to S2 (Feekes9) of the 2020–2021 growing season. Values are means ± SD (n = 3). Different lowercase letters denote significant differences (ANOVA, Fisher's least significant difference test, $P < 0.05$).

Table 2
Transportation ratio of ^{13}C photosynthate from the jointing stage (6 h after labeling) to the booting stage (9 d after labeling) in wheat organs.

Cultivars	Treatments	Treatment combination	Spike (%)	Leaf (%)	Stem (%)	Sheath (%)
CH58	WW	WW-C	50.32b	12.41a	-23.09b	6.44a
	MD	MD-C	47.33b	6.61a	-26.92bc	9.39a
	SD	SD-C	45.65b	3.43a	-43.15c	13.54a
LH6	WW	WW-L	58.13b	12.23a	-32.95bc	-31.70c
	MD	MD-L	59.33a	-25.97b	-6.37a	-13.84b
	SD	SD-L	42.53b	-27.29b	-3.27a	-13.99b
ANOVA	Cultivar (C)		*	* *	* *	* *
	Treatment (T)		* *	* *	*	*
	C×T		*	*	* *	ns

Note: WW, MD and SD represent well-water condition (as the control group), moderate drought and severe drought stress treatment, respectively, from booting to heading stage. Data were from the 2020-2021 growing season. Different lowercase letters denote significant differences at 0.05 levels. * and ** indicate significance at the $P < 0.05$ and 0.01 levels, respectively; ns, no significant difference.

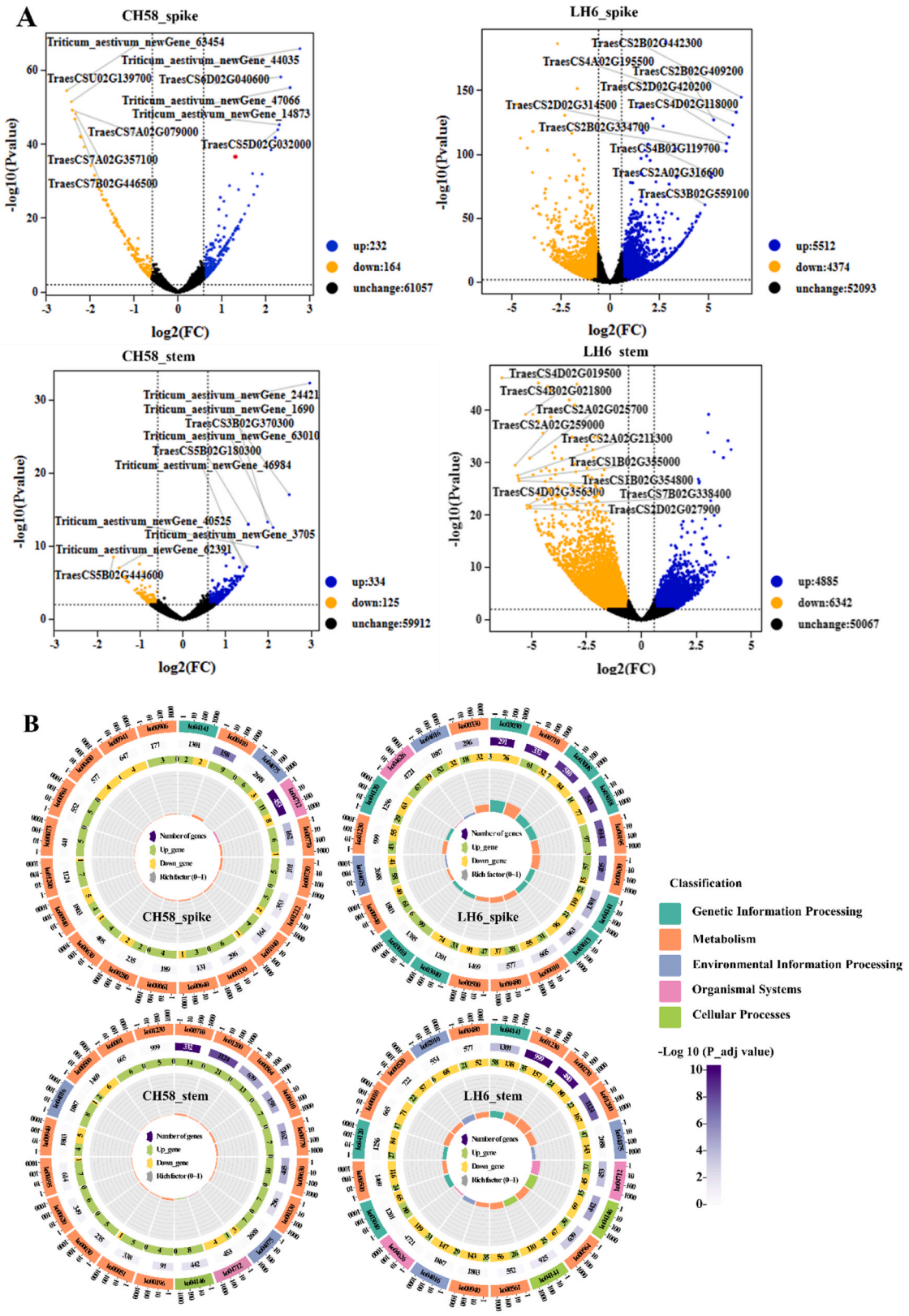

Fig. 6. Analysis of differentially expressed genes (DEGs) and enriched pathways in young spikes and stems of S2 (Feekes9). (A) Volcano diagrams of DEGs for WW vs SD of CH58_Spike, CH58_Stem, LH6_Spike and LH6_Stem. (B) KEGG pathway enrichment analysis of the DEGs by P–adj value. The first lap indicates the top 20 KEGG pathways, which were assigned to five main categories: genetic information processing, metabolism, environmental information processing, cellular processes, and organismal systems. The second lap indicates the number of this category in the background gene and -Log10P-adj values for gene enrichment for the specified category. The third lap indicates the number of genes that were upregulated (light green) and downregulated (yellow) in the specified category. The fourth lap represents the rich factor value of each category, and each cell of the background auxiliary line represents 0.1.

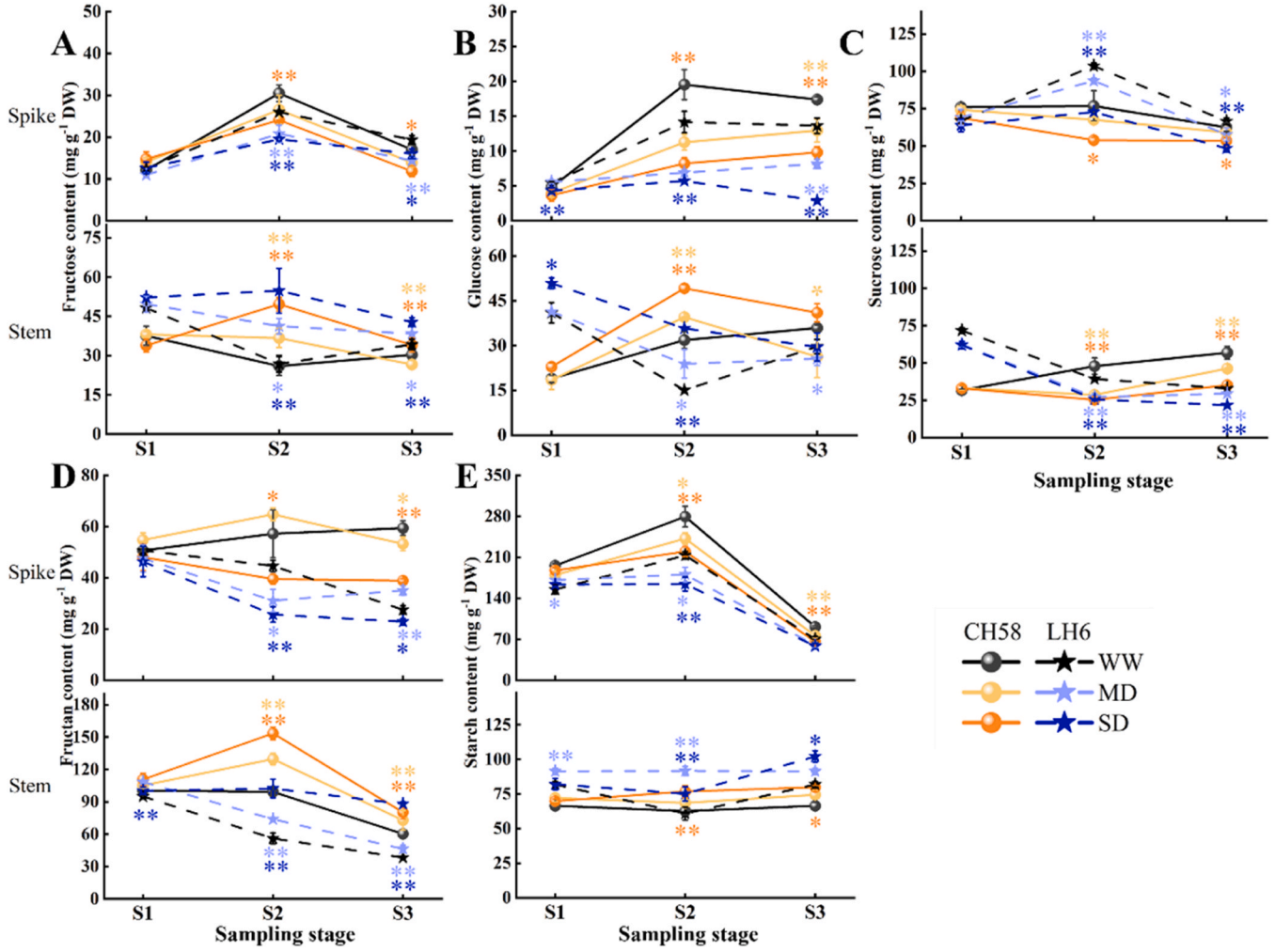

Fig. 7. Fructose (A), glucose (B), sucrose (C), fructan (D) and starch (E) concentrations in the spike and stem under different treatments. S1: the jointing stage (Feekes8) (the flag leaf tip was 2–4 cm); S2: the booting stage (Feekes9) (the wheat flag leaf pillow emerged 4–6 cm); and S3 (Feekes10.5): the heading stage (the spike of wheat emerged 4–6 cm). The data for A-E were from the 2020–2021 growing season. Values are means ± SD (n = 3). * and ** indicate significance at the $P < 0.05$ and 0.01 levels, respectively.

of LH6 under SD conditions. At the protein level, the activity of INV was higher in young spikes of CH58 at the S2 and S3 stages. In response to drought, the activities of INV and CWIN were significantly increased in the young ears and stems of CH58, as well as in the stems of LH6, while they were inhibited in the spikes of LH6 (Fig. 9).

For starch synthesis and decomposition, the expression of genes encoding SS, AGP, and alpha mylase (AMY) was upregulated in the young spikes and stems of CH58. However, *AGP* and beta-amylase (*BMY*) in the spike of LH6 were upregulated, while *AGP* and *AMY* were downregulated in the stem of CH58. Drought also changed the synthesis and decomposition of fructan. Specifically, MD and SD significantly increased the activity of FEH in the young spikes of CH58 and stems of LH6 at S2 and S3 but significantly decreased the activity of FEH in the spikes of LH6 and stems of CH58. Under SD conditions, the activity of SST was increased in the stems of both cultivars (Fig. 9).

The sucrose transport protein (*SUC/SUT)* and sugar final output protein *(SWEET)* in the spike of CH58 were upregulated under SD treatment but downregulated in the spike of LH6. The *SUC/SUT* and *SWEET* of both cultivars were upregulated in the stem by drought, and the upregulation of CH58 was higher than that of LH6 (Fig. 8B). However, the response of *STP* in the spikes of the two cultivars to drought was opposite, with upregulation in CH58 but downregulation in LH6. In the stem, the downregulation of *STP* in LH6 was more pronounced than that in CH58 (Fig. 8B). Therefore, after severe drought, the sugar unloading capacity of spikes of CH58 and the sugar loading capacity of stems were stronger than those of LH6.

3.7. Endogenous spermidine content and the number of fertile florets and sugar content after exogenous spermidine application

We also observed that a large number of DEGs in young spikes were enriched in the arginine and proline synthesis (Fig. 6B; Table S2) and that arginine was a biosynthetic precursor of polyamines. Therefore, we further determined the content of the major form of polyamine (spermidine) in young spikes. The results showed that compared to WW, drought stress (MD and SD) significantly reduced endogenous spermidine content in young wheat spikes at S2 and S3 (Fig. 10A). Interestingly, compared to SD, exogenous spermidine (SD-Spd) effectively increased the number of fertile florets under drought stress (Fig. 10B). Further analysis of sugar status in young spikes and stems showed that SD-Spd significantly increased fructose, glucose, and sucrose contents in young spikes at S2, as well as fructose and sucrose contents in young spikes at S3, especially in LH6 (Fig. 10C). Meanwhile, SD-Spd decreased fructose and glucose but increased sucrose content in LH6 stems under drought stress (Fig. 10C). Therefore, exogenous Spd application altered sugar partitioning in young spikes and stems and affected the number of fertile florets.

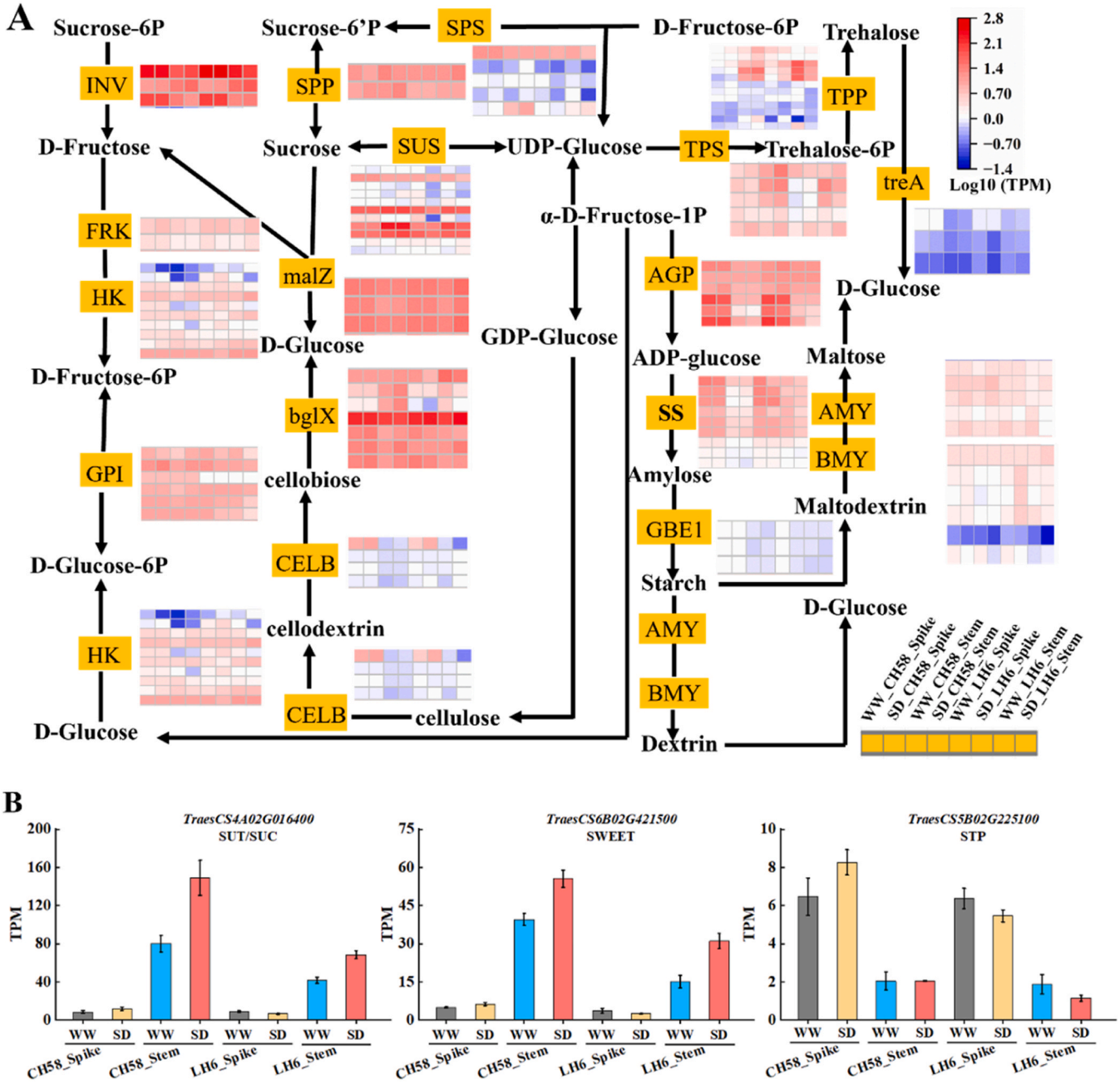

Fig. 8. Starch and sucrose metabolism (A) and sugar transporter protein-encoding gene expression (B) in young spikes and stems of CH58 and LH6 under different treatments. The heatmap shows the expression levels (Log10(TPM)) of genes involved in sucrose and starch metabolism. The transporter proteins and transcription factors are represented in yellow rectangles, whereas metabolites are displayed in bold black text. Detailed information on some featured genes involved in sucrose and starch metabolism in different organs is presented in Table S3. INV, betafructofuranosidase; HK, hexokinase; FRK, fructokinase; malZ, alpha-glucosidase; bglX, beta-glucosidase; CELB, cellulase; GPI, glucose-6-phosphate isomerase; SPP, sucrose-phosphate phosphatase; SPS, sucrose-phosphate synthase; SUS, sucrose synthase; AGP, ADP-glucose pyrophosphatase; SS, starch synthase; GBE1, 1,4-alpha-glucan branching enzyme; TPS, trehalose 6-phosphate synthase; TPP, trehalose 6-phosphate phosphatase; treA, alpha, alpha-trehalase; AMY, alpha-amylase; BMY, beta-amylase. SUC/SUT: sucrose transport protein; SWEET: sugar final output protein; STP: sugar transporter protein.

4. Discussion

4.1. *Drought inhibits the photosynthetic assimilation capacity of leaves to provide fewer assimilates for sinks*

The present study focuses on the changes in water content and storage capacity of the 0–100 cm soil layer from the jointing stage to the heading stage. As the soil textures were sandy loam (in the top) and clay loam (at the bottom), the 20–80 cm layer has the highest water storage capacity (Fig. 2). With the consumption of soil moisture, drought stress in the pre-reproductive stage mainly inhibits the formation of wheat grain number per spike but has little impact on spike number and thousand-grain weight (Ji et al., 2010; Zhang et al., 2020; Gao et al., 2023). In this study, moderate and severe drought significantly reduced the number of fertile florets and grains per spike of CH58 and LH6 (Table 1). Under severe drought, the degradation rate of florets of LH6 was higher (Table 1), which is related to the inhibition of leaf photosynthetic capacity by drought stress (Fig. S4). The accumulation of photosynthetic assimilates in leaves (sources) is the main source of carbohydrates for spike (sink) development (Tang et al., 2023; Shen

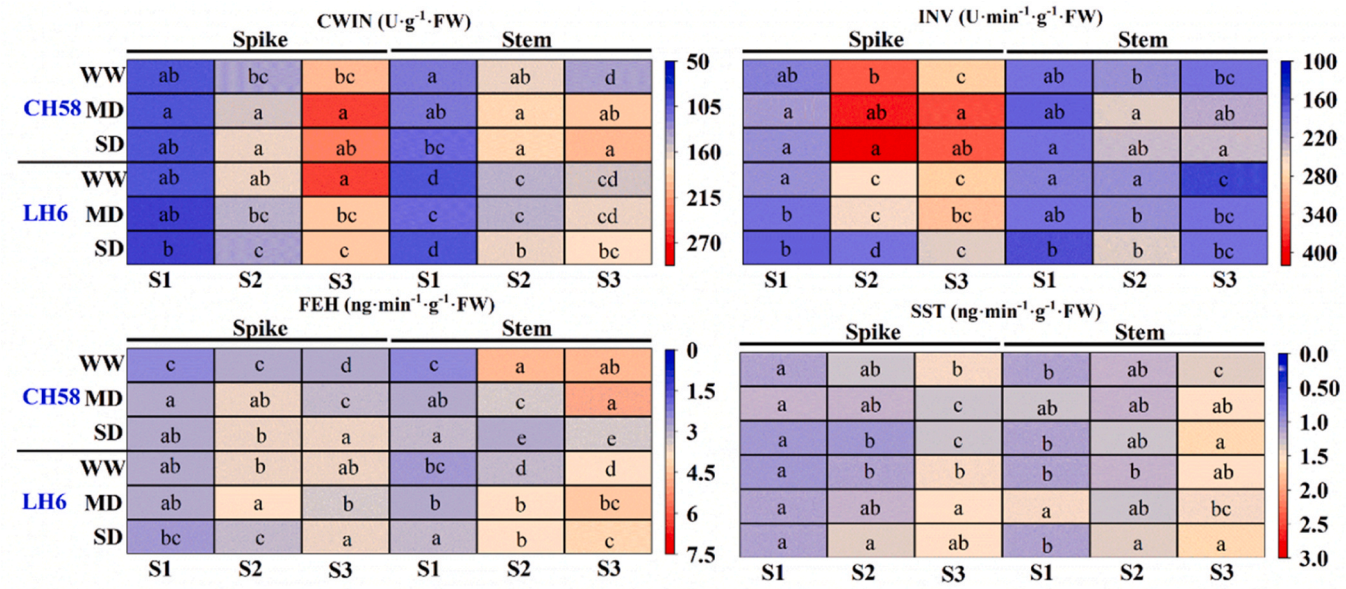

Fig. 9. Invertase and fructan synthase activities in the spike and stem under different treatments. CWIN: cell wall invertase; INV: soluble vacuolar invertase; FEH: 1-fructan exohydrolase; SST: sucrose: sucrose 1-fructosyl-transferase. S1: the jointing stage (Feekes8) (the flag leaf tip was 2–4 cm); S2: the booting stage (Feekes9) (the wheat flag leaf pillow emerged 4–6 cm); and S3 (Feekes10.5): the heading stage (the spike of wheat emerged 4–6 cm). The data were from the 2021–2022 growing season. Values are means (n = 3). Different lowercase letters denote significant differences (ANOVA, Fisher's least significant difference test, $P < 0.05$).

et al., 2023). However, our results showed that drought stress during booting significantly reduced the relative water content and chlorophyll content of leaves, thereby significantly reducing wheat Pn, Tr, and Gs (Fig. 3), which is consistent with the results of Song et al. (2018) and Kang et al. (2023). This is because (1) drought inhibits the activities of SOD, POD, and CAT, damages the antioxidant enzyme system, leads to ROS outbreaks in cells, and disrupts the stability of biofilms and proteins (Fig. 4; Rane et al., 2021); and (2) severe drought causes severe damage to the thylakoid grana and photosynthetic proteins of chloroplasts, leading to a decrease in light harvesting capacity (Kang et al., 2023). As photosynthetic capacity decreases, plant growth is inhibited, and dry matter accumulation significantly decreases (Fig. 5A), which marks the beginning of poor reproductive organ development.

4.2. *Assimilate allocation strategies related to drought resistance in spikes and stems affect the degradation of wheat florets*

The distribution of assimilates has a significant impact on plant growth, competition, and structural formation and is crucial for the development of plant reproductive organs (Li et al., 2019). Under water scarcity conditions, the allocation of assimilates in spikes and stems is jointly influenced by organ sensitivity to drought and differences in plant drought resistance (Ji et al., 2010; Cai et al., 2023). In this study, drought significantly inhibited the ^{13}C-photosynthates in the spike, leaf, stem, and sheath, and the degree of inhibition in LH6 was greater (Fig. 5B). Young spikes are the most sensitive organs to water scarcity (Danilevskaya et al., 2019), and even mild drought can easily lead to an insufficient supply of assimilates in the spikes and irreversible floret degradation (especially in drought-sensitive varieties) (Dolferus et al., 2011). Assimilates in spikes originate from long-distance transport in leaves, stems and sheaths (Zhao et al., 2022). Thus, floret degradation is closely related to the assimilate transfer rate of the organ. Interestingly, the transport of assimilates in the stems of two varieties with different drought resistance (CH58 and LH6) showed an opposite linear relationship with floret degradation (Fig. 5D). RNA-Seq results help explain this phenomenon, and the results showed that the number of DEGs in young spikes and stems of LH6 was significantly higher than that of CH58 under drought stress conditions (Fig. 6A). Previous studies have also observed that an increase in the number of DEGs in organs may lead to a rapid decrease in the number of grains (Bhardwaj et al., 2013; Sapeta et al., 2016). Therefore, the allocation strategies of assimilates in the spike and stem of wheat with different drought resistance affect the degradation of wheat florets.

4.3. *The great ability of spikes to utilize sugar and stems to transport sugar helps to resist the decrease in grain number per ear under drought stress*

A large number of DEGs in young spikes and stems were enriched in carbohydrate metabolism-related pathways, and LH6 had more DEGs than CH58 in sucrose and starch metabolism pathways (Fig. 6B). Ghiglione et al. (2008) found that excellent development of wheat florets was associated with increased sugar concentration in the growing spike. In this study, the contents of glucose, fructose, sucrose and starch in young spikes were positively correlated with the number of fertile florets and grains per spike and negatively correlated with the rate of floret degeneration (Fig. S7A). Glucose and fructose are produced from the breakdown of sucrose catalysed by the enzymes invertase (INV) and sucrose synthase (SuSy) (Ayre, 2011). Consistent with Zhang et al. (2020), drought significantly reduced the concentrations of sucrose, fructose and glucose in young spikes (Fig. 7A-C). Notably, drought induced relatively high INV enzyme activity and significant upregulation of the sucrose catabolism enzyme-encoding gene INV in young spikes of CH58 (Fig. 9; Fig. 8A). This may be the cause of the higher decrease in fructose and glucose concentrations in LH6 than in CH58 during the S2 period. However, severe drought downregulated *SUC/SUT* and *SWEET* expression in LH6 spikes but upregulated *SUC/SUT*, *SWEET and STP* expression in CH58 spikes (Fig. 8B), which is a compensatory pathway for low sucrose content in young CH58 spikes. The expression of sugar transporter proteins and convertase activity in spikes were positively correlated with the number of fertile florets (Fig. S7B). The involvement of *OsSUT2* and *OsSWEET4* has also been found in rice to synergistically regulate the number of grains per spike (Sun et al., 2023). Moreover, meiotic drought-induced reductions in invertase activity and changes in starch metabolism-related enzymes tend to cause starch synthesis deficiencies and pollen development disruption (Jin et al., 2013). In this study, drought upregulated the expression of *AGP*, *AMY* and *BMY*, leading to a significant decrease in starch content in young

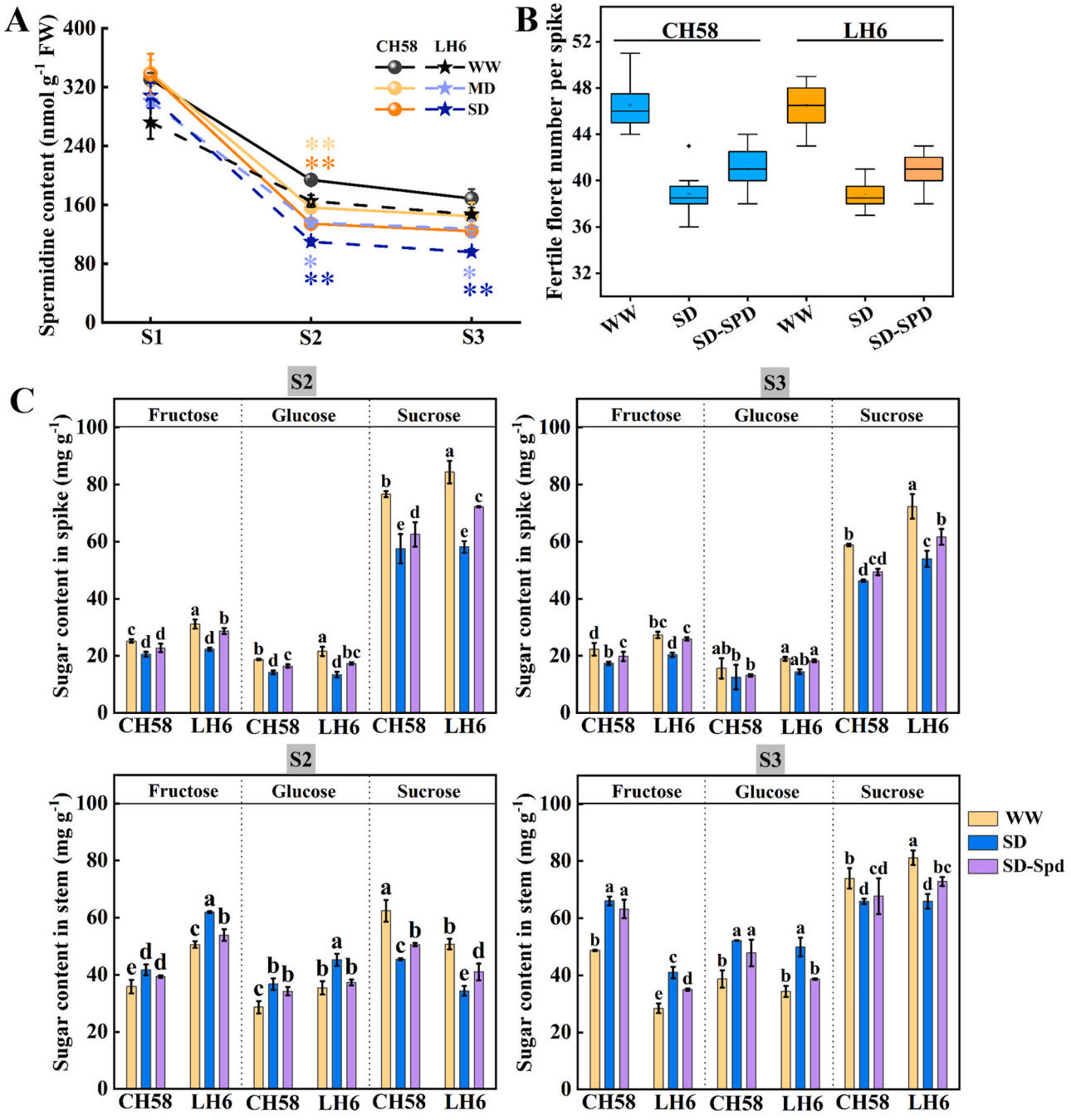

Fig. 10. Endogenous spermidine content (A), number of fertile florets (B), and fructose, glucose and sucrose concentrations in spikes and stems (C). S1: the jointing stage (Feekes8) (the flag leaf tip was 2–4 cm); S2: the booting stage (Feekes9) (the wheat flag leaf pillow emerged 4–6 cm); and S3 (Feekes10.5): the heading stage (the spike of wheat emerged 4–6 cm). The data for A were from the 2021–2022 growing season of Experiment I. Values are means ± SD (n = 3).The data for B-C were from the 2021–2022 growing season of Experiment II. Values are means ± SD (n = 12 (B) and 3 (C)). * and ** indicate significance at the $P < 0.05$ and 0.01 levels, respectively. Different lowercase letters denote significant differences (ANOVA, Fisher's least significant difference test, $P < 0.05$).

spikes (Fig. 7E and Fig. 8A), which may also explain the abortion rate of florets (Table 1). Overall, the superior sucrose unloading and utilization capacity in young spikes of CH58 is beneficial for the formation of grain number under water deficit stress.

Sugar metabolism and sugar transporters in the stem, which serves as a support and transport organ for the uptake of assimilates from the roots and leaves to the spike, play an important role in the uptake and transport of assimilates in the spike (Dreccer et al., 2009; Gautam et al., 2022). The main form of transport of assimilates from photosynthetic organs to reproductive organs in plants is sucrose (Greco et al., 2012). The sucrose in reproductive organs is transported by starch and fructans stored in the stems and sheaths after first hydrolysing them to single sugars and then resynthesizing sucrose (Ayre et al., 2011; Shen et al., 2018). In this study, the MD and SD treatments significantly reduced the sucrose content in stems, and notably, the reduction was higher in CH58 than in LH6 (Fig. 7C). For this, we hypothesized that (1) a large amount of sucrose in CH58 stems might be catabolized to hexose or (2) some of the sucrose in CH58 stems might be transported via the phloem to the young spike. Although the hexose content in stems was enhanced after drought, the increase was significantly higher in LH6 stems in the SD treatment than in CH58 stems (Fig. 7A-B). In addition, high expression of *SUT/SUC* and *SWEET* was observed in CH58 stems, and higher levels

of expression were observed after exposure to drought (Fig. 8B). Therefore, the latter hypothesis is confirmed. On the other hand, the second internode under the spike of CH58 under SD conditions had a larger vascular bundle area and provided structural support for more sucrose transportation from the phloem to the spike (Fig. S8).

Fructans not only have an indirect role as hexose reserves but also work as osmotic substances to directly protect tissues from damage caused by abiotic stresses such as drought and low temperature (Livingston et al., 2009). When exposed to severe drought, the fructan content in young spikes of CH58 and LH6 was significantly decreased (Fig. 7D). The fructan content in wheat stems is strongly influenced by genotype (Dreccer et al., 2009). Drought stress affects the expression of genes related to fructan synthesis and catabolism (e.g., *1-SST*, *1-FEH*, *6-SFT*), which synergistically regulate fructan accumulation in wheat stems (Hou et al., 2018). The concentrations of fructan in the stems of S2 and S3 increased significantly after SD treatment, and the increase was more significant in CH58 than in LH6 (Fig. 7D). This may be a consequence of FEH in CH58 stems being inhibited but enhanced in LH6 by drought when SST was upregulated by drought in both varieties (Fig. 9). The relatively sufficient fructans in the stems under drought also provide source material and energy for sucrose translocation from stems to spikes. Furthermore, starch reutilization in stems provides energy and carbon support for the early development of reproductive organs (Scofield et al., 2009), and drought caused starch in stems to first increase and then decrease by drought, which did not significantly differ between the two cultivars (Fig. 7E). Thus, the reutilization efficiency of starch in the stems of both cultivars may not be as strongly related to drought tolerance as that of fructans.

4.4. Exogenous spermidine effectively improves spike-stem sugar distribution under drought and thus promotes the formation of fertile florets in wheat

Spermidine is a major form of polyamine (a general term for low molecular weight aliphatic nitrogen-containing bases) and is regarded as a growth regulator or second messenger of hormones (Davies, 2004; Yang et al., 2007), which frequently interacts with ethylene to regulate wheat floret degradation (Lyu et al., 2016; Zhang et al., 2017). In this study, endogenous spermidine was significantly reduced in young spikes under drought stress (Fig. 10A), and the endogenous spermidine content was significantly and positively correlated with the number of fertile florets. Exogenous spermidine promotes the formation of fertile florets and increases the number of grains per spike under stress conditions such as drought and salt stress (Chunthaburee et al., 2015; Zhang et al., 2017). A similar result was obtained in our study (Fig. 10B), and the promoting effect was more prominent in the weakly drought-resistant cultivar. High concentrations of hexose can be utilized directly to provide nutrients for the development of sink organs (Guan et al., 2023). Meanwhile, exogenous spermidine increased the sucrose content in LH6 stems under drought stress (Fig. 10C), and more sucrose in the stems would provide a better physical basis for sugar transport to the spike (Willenbrink et al., 2008). Therefore, exogenous chemicals can promote the formation of fertile florets by enhancing the distribution status of assimilates in the spike and stem, thereby reducing the negative impact of drought on the formation of grain numbers.

5. Conclusion

Pre-reproductive drought inhibits photosynthesis of leaves and assimilate partitioning between spikes and stems to increase the rate of floret degradation and abortion, which leads to a reduction in the number of fertile florets and grains in wheat. Under drought stress, compared to LH6, CH58 (more drought tolerant) had greater sugar catabolism and sugar unloading capacity in young spikes, as well as higher fructan content and sugar loading capacity in the stems, which provide more assimilates for the process of floret development to relieve the negative impacts of drought on the formation of grain number in spikes. Therefore, the ability of the spike to utilize sugar and the difference in competition for assimilates between the spike and stem determine the degree of inhibition of drought on the formation of grain numbers. Exogenous spermidine optimizes sugar distribution in the panicle and stem and promotes the smooth formation of fertile florets under drought stress. This study provides new insights for reducing wheat yield loss under climate change and guiding the breeding of drought-resistant wheat varieties.

Funding

This work was supported by the National Natural Science Foundation of China (31871567) and the Key Research and Development Program of Shaanxi (2021NY-083).

CRediT authorship contribution statement

Liu Yang: Funding acquisition, Supervision, Writing – review & editing. **Li Juan:** Conceptualization, Investigation, Writing – original draft. **Liang Zimeng:** Conceptualization, Investigation, Writing – review & editing. **Li Yakun** and **Wang Kexin:** Formal analysis, Investigation. **Nangia Vinay:** Conceptualization, Supervision, Visualization. **Mo Fei:** Conceptualization, Supervision, Visualization.

Declaration of Competing Interest

The authors declare that they have no known competing financial interests or personal relationships that could have appeared to influence the work reported in this paper.

Data availability

The authors do not have permission to share data.

Acknowledgements

We thank Hongxia Li and Maomao Wang from the Crop Biology Innovation Center for their help in the determination of spermidine and sugar components by High-performance Liquid Chromatography.

Appendix A. Supporting information

Supplementary data associated with this article can be found in the online version at doi:10.1016/j.agwat.2024.108675.

References

Ayre, B.G., 2011. Membrane-transport systems for sucrose in relation to whole-plant carbon partitioning. Mol. Plant 4, 377–394.
Barnabas, B., Jager, K., Feher, A., 2008. The effect of drought and heat stress on reproductive processes in cereals. Plant Cell Environ. 31, 11–38.
Bavnhoj, L., Paulsen, P.A., Flores-Canales, J.C., Schiott, B., Pedersen, B.P., 2021. Molecular mechanism of sugar transport in plants unveiled by structures of glucose/H(+) symporter STP10. Nat. Plants 7, 1409–1419.
Bhardwaj, J., Chauhan, R., Swarnkar, M.K., Chahota, R.K., Singh, A.K., Shankar, R., Yadav, S.K., 2013. Comprehensive transcriptomic study on horse gram (Macrotyloma uniflorum): de novo assembly, functional characterization and comparative analysis in relation to drought stress. BMC Genom. 14, 647.
Cai, F., Mi, N., Ming, H., Zhang, Y., Zhang, H., Zhang, S., Zhao, X., Zhang, B., 2023. Responses of dry matter accumulation and partitioning to drought and subsequent rewatering at different growth stages of maize in Northeast China. Front Plant Sci. 14, 1110727.
Chunthaburee, S., Sanitchon, J., Pattanagul, W., Theerakulpisut, P., 2015. Effects of salt stress after late booting stage on yield and antioxidant capacity in pigmented rice grains and alleviation of the salt-induced yield reduction by exogenous spermidine. Plant Prod. Sci. 18, 32–42.
Clement, C., Audran, J.C., 1995. Anther wall layers control pollen sugar nutrition in Lilium. Protoplasma 187, 172–181.

Danilevskaya, O.N., Yu, G., Meng, X., Xu, J., Stephenson, E., Estrada, S., Chilakamarri, S., Zastrow-Hayes, G., Thatcher, S., 2019. Developmental and transcriptional responses of maize to drought stress under field conditions. Plant Direct 3, e00129.
Davies, P.J., 2004. The plant hormones: their nature, occurrence and function. In: Davies, P.J. (Ed.), Plant Hormones, Biosynthesis, Signal Transduction, Action. Kluwer Academic Publishers, Dordrecht, pp. 1–15.
Dolferus, R., Ji, X., Richards, R.A., 2011. Abiotic stress and control of grain number in cereals. Plant Sci. 181, 331–341.
Dong, B., Zheng, X., Liu, H., Able, J.A., Yang, H., Zhao, H., Zhang, M., Qiao, Y., Wang, Y., Liu, M., 2017. Effects of drought stress on pollen sterility, grain yield, abscisic acid and protective enzymes in two winter wheat cultivars. Front Plant Sci. 8, 1008.
Dreccer, M.F., Herwaarden, A.F., Chapman, S.C., 2009. Grain number and grain weight in wheat lines contrasting for stem water soluble carbohydrate concentration. Field Crop Res. 112, 43–54.
Dreccer, M.F., Wockner, K.B., Palta, J.A., McIntyre, C.L., Borgognone, M.G., Bourgault, M., Reynolds, M., Miralles, D.J., 2014. More fertile florets and grains per spike can be achieved at higher temperature in wheat lines with high spike biomass and sugar content at booting. Funct. Plant Biol. 41, 482–495.
Durand, M., Porcheron, B., Hennion, N., Maurousset, L., Lemoine, R., Pourtau, N., 2016. Water deficit enhances C export to the roots in arabidopsis thaliana plants with contribution of sucrose transporters in both shoot and roots. Plant Physiol. 170, 1460–1479.
Feekes, W., 1941. De tarwe en haar milieu. Versl. techn.Tarwe Comm. 12, 523–888.
Fischer, R.A., 2011. Wheat physiology: a review of recent developments. Crop Pasture Sci. 62, 95–114.
Gao, J., Zhang, Y., Xu, C., Wang, X., Wang, P., Huang, S., 2023. Abscisic acid collaborates with lignin and flavonoid to improve pre-silking drought tolerance by tuning stem elongation and ear development in maize (Zea mays L.). Plant J. 114, 437–454.
Gautam, T., Dutta, M., Jaiswal, V., Zinta, G., Gahlaut, V., Kumar, S., 2022. Emerging roles of SWEET sugar transporters in plant development and abiotic stress responses. Cells 11.
Ghiglione, H.O., Gonzalez, F.G., Serrago, R., Maldonado, S.B., Chilcott, C., Cura, J.A., Miralles, D.J., Zhu, T., Casal, J.J., 2008. Autophagy regulated by day length determines the number of fertile florets in wheat. Plant J. 55, 1010–1024.
Greco, M., Chiappetta, A., Bruno, L., Bitonti, M.B., 2012. In Posidonia oceanica cadmium induces changes in DNA methylation and chromatin patterning. J. Exp. Bot. 63, 695–709.
Guan, X., Zhang, Y., Zhou, L., Asad, M.A.U., Zhao, Q., Pan, G., Cheng, F., 2023. Disruptions of sugar utilization and carbohydrate metabolism in rice developing anthers aggravated heat stress-induced pollen abortion. Plant Physiol. Biochem 202, 107991.
Guo, Z., Slafer, G.A., Schnurbusch, T., 2016. Genotypic variation in spike fertility traits and ovary size as determinants of floret and grain survival rate in wheat. J. Exp. Bot. 67, 4221–4230.
Gupta, A., Rico-Medina, A., Caño-Delgado, A.I., 2020. The physiology of plant responses to drought. Science 368, 266–269.
Hanft, J.M., Jones, R.J., 1986. Kernel abortion in maize: I. Carbohydrate concentration patterns and acid invertase activity of maize kernels induced to abort in vitro. Plant Physiol. 81, 503–510.
He, J., Hu, W., Li, Y., Zhu, H., Zou, J., Wang, Y., Meng, Y., Chen, B., Zhao, W., Wang, S., Zhou, Z., 2022. Prolonged drought affects the interaction of carbon and nitrogen metabolism in root and shoot of cotton. Environ Exp Bot 197.
Hodges, D.M., DeLong, J.M., Forney, C.F., Prange, R.K., 1999. Improving the thiobarbituric acid-reactive-substances assay for estimating lipid peroxidation in plant tissues containing anthocyanin and other interfering compounds. Planta 207, 604–611.
Hou, J., Huang, X., Sun, W., Du, C., Wang, C., Xie, Y., Ma, Y., Ma, D., 2018. Accumulation of water-soluble carbohydrates and gene expression in wheat stems correlates with drought resistance. J. Plant Physiol. 231, 182–191.
Hu, W., Huang, Y., Loka, D.A., Bai, H., Liu, Y., Wang, S., Zhou, Z., 2020. Drought-induced disturbance of carbohydrate metabolism in anthers and male abortion of two Gossypium hirsutum cultivars differing in drought tolerance. Plant Cell Rep. 39, 195–206.
Hunt Jr., E.R., Rock, B.N., Nobel, P.S., 1987. Measurement of leaf relative water content by infrared reflectance. Remote Sens. Environ. 22, 429–435.
Inoue, T., Inanaga, S., Sugimoto, Y., El Siddig, K., 2004. Contribution of pre-anthesis assimilates and current photosynthesis to grain yield, and their relationships to drought resistance in wheat cultivars grown under different soil moisture. Photosynthetica 42, 99–104.
Ji, X., Shiran, B., Wan, J., Lewis, D.C., Jenkins, C.L., Condon, A.G., Richards, R.A., Dolferus, R., 2010. Importance of pre-anthesis anther sink strength for maintenance of grain number during reproductive stage water stress in wheat. Plant Cell Environ. 33, 926–942.
Jiang, M., Zhang, J., 2002. Water stress-induced abscisic acid accumulation triggers the increased generation of reactive oxygen species and up-regulates the activities of antioxidant enzymes in maize leaves. J. Exp. Bot. 53, 2401–2410.
Jiang, N., Yu, P., Fu, W., Li, G., Feng, B., Chen, T., Li, H., Tao, L., Fu, G., 2020. Acid invertase confers heat tolerance in rice plants by maintaining energy homoeostasis of spikelets. Plant Cell Environ. 43, 1273–1287.
Jin, Y., Yang, H., Wei, Z., Ma, H., Ge, X., 2013. Rice male development under drought stress: phenotypic changes and stage-dependent transcriptomic reprogramming. Mol. Plant 6, 1630–1645.
Kang, J., Chu, Y., Ma, G., Zhang, Y., Zhang, X., Wang, M., Lu, H., Wang, L., Kang, G., Ma, D., Xie, Y., Wang, C., 2023. Physiological mechanisms underlying reduced photosynthesis in wheat leaves grown in the field under conditions of nitrogen and water deficiency. Crop J. 11, 638–650.
Kaur, H., Manna, M., Thakur, T., Gautam, V., Salvi, P., 2021. Imperative role of sugar signaling and transport during drought stress responses in plants. Physiol. Plant 171, 833–848.
Khoshro, H.H., Taleei, A., Bihamta, M.R., Shahbazi, M., Abbasi, A., Ramezanpour, S.S., 2014. Expression analysis of the genes involved in accumulation and remobilization of assimilates in wheat stem under terminal drought stress. Plant Growth Regul. 74, 165–176.
Lemoine, R., La Camera, S., Atanassova, R., Dedaldechamp, F., Allario, T., Pourtau, N., Bonnemain, J.L., Laloi, M., Coutos-Thevenot, P., Maurousset, L., Faucher, M., Girousse, C., Lemonnier, P., Parrilla, J., Durand, M., 2013. Source-to-sink transport of sugar and regulation by environmental factors. Front Plant Sci. 4, 272.
Li, B., Ruotti, V., Stewart, R.M., Thomson, J.A., Dewey, C.N., 2010. RNA-Seq gene expression estimation with read mapping uncertainty. Bioinformatics 26, 493–500.
Li, J., Li, Q., Guo, N., Xian, Q., Lan, B., Vinay, N., Mo, F., Liu, Y., 2023. Polyamines mediate the inhibitory effect of drought stress on nitrogen reallocation and utilization to regulate the grain number in wheat. J. Exp. Bot., erad393
Li, W., Zhang, H., Huang, G., Liu, R., Wu, H., Zhao, C., McDowell, N.G., Field, R., 2019. Effects of nitrogen enrichment on tree carbon allocation: a global synthesis. Glob. Ecol. Biogeogr. 29, 573–589.
Liang, Z., Luo, J., Wei, B., Liao, Y., Liu, Y., 2021. Trehalose can alleviate decreases in grain number per spike caused by low-temperature stress at the booting stage by promoting floret fertility in wheat. J. Agron. Crop Sci. 207, 717–732.
Liu, M., Ouyang, S., Tian, Y., Wen, S., Zhao, Y., Li, X., Baoyin, T.T., Kuzyakov, Y., Xu, X., 2020. Effects of rotational and continuous overgrazing on newly assimilated C allocation. Biol. Fert. Soils 57, 193–202.
Liu, Y., Liang, H., Lv, X., Liu, D., Wen, X., Liao, Y., 2016. Effect of polyamines on the grain filling of wheat under drought stress. Plant Physiol. Bioch 100, 113–129.
Liu, Z., Sha, Y., Huang, Y., Hao, Z., Guo, W., Ke, L., Chen, F., Yuan, L., Mi, G., 2022. Efficient nitrogen allocation and reallocation into the ear in relation to the superior vascular system in low-nitrogen tolerant maize hybrid. Field Crop Res. 284.
Livingston 3rd, D.P., Hincha, D.K., Heyer, A.G., 2009. Fructan and its relationship to abiotic stress tolerance in plants. Cell Mol. Life Sci. 66, 2007–2023.
Lobell, D.B., Roberts, M.J., Schlenker, W., Braun, N., Little, B.B., Rejesus, R.M., Hammer, G.L., 2014. Greater sensitivity to drought accompanies maize yield increase in the U.S. Midwest. Science 344, 516–519.
Lyu, X.K., Wen, X.X., Liao, Y.C., Liu, Y., 2016. Effect of exogenous polyamines on mechanism of floret degeneration in wheat. Acta Agron. Sin. 42.
Maehly, A.C., Chance, B., 1955. The assay of catalases and peroxidases. Method Enzym. 2, 764–775.
Mathan, J., Singh, A., Ranjan, A., 2021. Sucrose transport in response to drought and salt stress involves ABA-mediated induction of OsSWEET13 and OsSWEET15 in rice. Physiol. Plant 171, 620–637.
Peshev, D., Van den Ende, W., 2014. Fructans: prebiotics and immunomodulators. J. Funct. Foods 8, 348–357.
Qin, J.X., Jiang, Y.J., Lu, Y.Z., Zhao, P., Wu, B.J., Li, H.X., Wang, Y., Xu, S.B., Sun, Q.X., Liu, Z.S., 2020. Genome-wide identification and transcriptome profiling reveal great expansion of SWEET gene family and their wide-spread responses to abiotic stress in wheat (*Triticum aestivum* L.). J. Integr. Agr. 19, 1704–1720.
Rane, J., Singh, A.K., Tiwari, M., Prasad, P.V.V., Jagadish, S.V.K., 2021. Effective use of water in crop plants in dryland agriculture: implications of reactive oxygen species and antioxidative system. Front Plant Sci. 12, 778270.
Rottmann, T., Fritz, C., Sauer, N., Stadler, R., 2018. Glucose uptake via STP transporters inhibits in vitro pollen tube growth in a HEXOKINASE1-dependent manner in Arabidopsis thaliana. Plant Cell 30, 2057–2081.
Ruan, Y.L., 2014. Sucrose metabolism: gateway to diverse carbon use and sugar signaling. Annu Rev Plant Biol 65, 33–67.
Santiago, J.P., Sharkey, T.D., 2019. Pollen development at high temperature and role of carbon and nitrogen metabolites. Plant Cell Environ. 42, 2759–2775.
Sapeta, H., Lourenco, T., Lorenz, S., Grumaz, C., Kirstahler, P., Barros, P.M., Costa, J.M., Sohn, K., Oliveira, M.M., 2016. Transcriptomics and physiological analyses reveal co-ordinated alteration of metabolic pathways in Jatropha curcas drought tolerance. J. Exp. Bot. 67, 845–860.
Scofield, G.N., Ruuska, S.A., Aoki, N., Lewis, D.C., Tabe, L.M., Jenkins, C.L., 2009. Starch storage in the stems of wheat plants: localization and temporal changes. Ann. Bot. 103, 859–868.
Sharma, P., Dubey, R.S., 2004. Ascorbate peroxidase from rice seedlings: properties of enzyme isoforms, effects of stresses and protective roles of osmolytes. Plant Sci. 167, 541–550.
Shen, S., Zhang, L., Liang, X.G., Zhao, X., Lin, S., Qu, L.H., Liu, Y.P., Gao, Z., Ruan, Y.L., Zhou, S.L., 2018. Delayed pollination and low availability of assimilates are major factors causing maize kernel abortion. J. Exp. Bot. 69, 1599–1613.
Shen, S., Liang, X.G., Zhang, L., Zhao, X., Liu, Y.P., Lin, S., Gao, Z., Wang, P., Wang, Z.M., Zhou, S.L., 2020. Intervening in sibling competition for assimilates by controlled pollination prevents seed abortion under postpollination drought in maize. Plant Cell Environ. 43, 903–919.
Shen, S., Ma, S., Wu, L., Zhou, S.L., Ruan, Y.L., 2023. Winners take all: competition for carbon resource determines grain fate. Trends Plant Sci. 28, 893–901.
Sheoran, S., Kaur, Y., Kumar, S., Shukla, S., Rakshit, S., Kumar, R., 2022. Recent advances for drought stress tolerance in maize (Zea mays L.): present status and future prospects. Front Plant Sci. 13, 872566.
Smith, A.M., Stitt, M., 2007. Coordination of carbon supply and plant growth. Plant Cell Environ. 30, 1126–1149.
Song, H., Li, Y., Zhou, L., Xu, Z., Zhou, G., 2018. Maize leaf functional responses to drought episode and rewatering. Agric. Meteor. 249, 57–70.
Sun, C., Wang, Y., Yang, X., Tang, L., Wan, C., Liu, J., Chen, C., Zhang, H., He, C., Liu, C., Wang, Q., Zhang, K., Zhang, W., Yang, B., Li, S., Zhu, J., Sun, Y., Li, W., Zhou, Y.,

Wang, P., Deng, X., 2023. MATE transporter GFD1 cooperates with sugar transporters, mediates carbohydrate partitioning and controls grain-filling duration, grain size and number in rice. Plant Biotechnol. J. 21, 621–634.
Tang, S., Li, L., Wang, Y., Chen, Q., Zhang, W., Jia, G., Zhi, H., Zhao, B., Diao, X., 2017. Genotype-specific physiological and transcriptomic responses to drought stress in Setaria italica (an emerging model for Panicoideae grasses). Sci. Rep. 7, 10009.
Tang, Y., Guo, J., Jagadish, S.V.K., Yang, S., Qiao, J., Wang, Y., Xie, K., Wang, H., Yang, Q., Deng, L., Shao, R., 2023. Ovary abortion in field-grown maize under water-deficit conditions is determined by photo-assimilation supply. Field Crop Res. 293.
Tian, G., Wang, S., Wu, J., Wang, Y., Wang, X., Liu, S., Han, D., Xia, G., Wang, M., 2023. Allelic variation of TaWD40-4B.1 contributes to drought tolerance by modulating catalase activity in wheat. Nat. Commun. 14, 1200.
Van den Ende, W., 2013. Multifunctional fructans and raffinose family oligosaccharides. Front Plant Sci. 4, 247.
Wang, B., Liu, C., Zhang, D., He, C., Zhang, J., Li, Z., 2019. Effects of maize organ-specific drought stress response on yields from transcriptome analysis. BMC Plant Biol. 19, 335.
Wang, L., Ruan, Y.L., 2012. New insights into roles of cell wall invertase in early seed development revealed by comprehensive spatial and temporal expression patterns of GhCWIN1 in cotton. Plant Physiol. 160, 777–787.
Wardlaw, I.F., Willenbrink, J., 1994. Carbohydrate storage and mobilization bythe culm of wheat between heading and grain maturity: the relation tosucrose synthase and sucrose-phosphate synthase. Aust. J. Plant Physiol. 21, 255–271.
Willenbrink, J., Bonnett, G.D., Willenbrink, S., Wardlaw, I.F., 2008. Changes of enzyme activities associated with the mobilization of carbohydrate reserves (fructans) from the stem of wheat during kernel filling. N. Phytol. 139, 471–478.
Wu, W.X., Liu, W., Lu, H.H., Chen, Y.X., Medha, D., Janice, T., 2009. Use of 13C labeling to assess carbon partitioning in transgenic and nontransgenic (parental) rice and their rhizosphere soil microbial communities. FEMS Microbiol. Ecol. 67, 93–102.
Xue, G.P., Kooiker, M., Drenth, J., McIntyre, C.L., 2011. TaMYB13 is a transcriptional activator of fructosyltransferase genes involved in beta-2,6-linked fructan synthesis in wheat. Plant J. 68, 857–870.
Yang, H., Li, Y., Qiao, Y., Sun, H., Liu, W., Qiao, W., Li, W., Liu, M., Dong, B., 2023. Low light stress promotes new tiller regeneration by changing source-sink relationship and activating expression of expansin genes in wheat. Plant Cell Environ. 46, 1562–1581.
Yang, J., Zhang, J., Liu, K., Wang, Z., Liu, L., 2007. Involvement of polyamines in the drought resistance of rice. J. Exp. Bot. 58, 1545–1555.
Yu, J., Jiang, M., Guo, C., 2019. Crop pollen development under drought: from the phenotype to the mechanism. Int. J. Mol. Sci. 20.
Zhang, J., Chen, W., Dell, B., Vergauwen, R., Zhang, X., Mayer, J.E., Van den Ende, W., 2015a. Wheat genotypic variation in dynamic fluxes of WSC components in different stem segments under drought during grain filling. Front Plant Sci. 6, 624.
Zhang, J., Xu, Y., Chen, W., Dell, B., Vergauwen, R., Biddulph, B., Khan, N., Luo, H., Appels, R., Van den Ende, W., 2015b. A wheat 1-FEH w3 variant underlies enzyme activity for stem WSC remobilization to grain under drought. N. Phytol. 205, 293–305.
Zhang, W., Chen, Y., Wang, Z., Yang, J., 2017. Polyamines and ethylene in rice young panicles in response to soil drought during panicle differentiation. Plant Growth Regul. 82, 491–503.
Zhang, Z., Huang, J., Gao, Y., Liu, Y., Li, J., Zhou, X., Yao, C., Wang, Z., Sun, Z., Zhang, Y., 2020. Suppressed ABA signal transduction in the spike promotes sucrose use in the stem and reduces grain number in wheat under water stress. J. Exp. Bot. 71, 7241–7256.
Zhang, Z., Li, J., Hu, N., Li, W., Qin, W., Li, J., Gao, Y., Liu, Y., Sun, Z., Yu, K., Wang, Z., Zhang, Y., 2021. Spike growth affects spike fertility through the number of florets with green anthers before floret abortion in wheat. Field Crop Res. 260.
Zhao, Y., Liang, C., Shao, S., Li, J., Xie, H., Zhang, W., Chen, F., He, H., Zhang, X., 2021. Interactive effects of elevated CO_2 and nitrogen fertilization levels on photosynthesized carbon allocation in a temperate spring wheat and soil system. Pedosphere 31, 191–203.
Zhao, Z., Wang, C., Yu, X., Tian, Y., Wang, W., Zhang, Y., Bai, W., Yang, N., Zhang, T., Zheng, H., Wang, Q., Lu, J., Lei, D., He, X., Chen, K., Gao, J., Liu, X., Liu, S., Jiang, L., Wang, H., Wan, J., 2022. Auxin regulates source-sink carbohydrate partitioning and reproductive organ development in rice. Proc. Natl. Acad. Sci. U. S. A. 119, e2121671119.
Zinselmeier, C., Jeong, B.R., Boyer, J.S., 1999. Starch and the control of kernel number in maize at low water potentials. Plant Physiol. 121, 25–36.